

Statistics of Merging Peaks of Random Gaussian Fluctuations: Skeleton Tree Formalism

Hitoshi HANAMI

Physics Section, Faculty of Humanities and Social Sciences, Iwate University, Morioka 020 JAPAN

Accepted 1999 August ?? Received 1999 July 14; in original form 1999 July 11

ABSTRACT

The cosmological bound objects were considered to form from the local maxima of cosmological density fluctuations; often assumed to be Gaussian random fields. In order to study the statistics of the objects with hierarchical merging, we propose *the skeleton tree formalism*, which can analytically distinguish the episodic merging and the continuous accretion in the mass growth processes. The distinction was not clear in extended Press-Schechter (PS) formalism. The skeleton tree formalism is a natural extension of the peak theory which is an alternative formalism for the statistics of the bound objects. The fluctuation field smoothing with Gaussian filter produces the landscape with adding the extra-dimension of the filter resolution scale to the spatial coordinate of the original fluctuation. In the landscape, some smoothing peaks are nesting into the neighboring peaks at a type of critical points called *sloping saddles* appears, which can be interpreted as merging events of the objects in the context of the hierarchical structure formation. The topological properties of the landscape can be abstracted in *skeleton trees*, which consist of line process of the smoothing peaks and the point process of the sloping saddles. According to this abstract topological picture, in this paper, we present the concept and the basic results of *the skeleton tree formalism* to describe (1) the distinction between the accretion and the merger in the hierarchical structure formation from various initial random Gaussian fields; (2) the instantaneous number density of the sloping saddles which gives the instantaneous scale function of the objects with the destruction and reformation in the mergers; (3) the rates of the destruction, the reformation, and the relative accretion growth; (4) the self-consistency of the formalism for the statistics of the mass growth processes of the objects; (5) the mean growth history of the objects at the fixed mass.

Key words: galaxies:clustering – galaxies:formation – cosmology:theory – dark matter

1 INTRODUCTION

Hierarchical clustering scenario, including the cold dark matter (CDM) model, may be the most established one for reconstructing various observational properties in the cosmological structure from the galaxies to the clusters of galaxies. Press & Schechter (1974) firstly proposed an analytical formalism which derives the number density of bound virialized objects of the mass at any given epoch, with the assumption that the primordial density fluctuations is random Gaussian field. The mass function predicted by the PS theory shows reasonably the good agreement with N-body simulations even if it has more low mass objects (e.g. Lacey & Cole 1994). To reconstruct the observational properties in theoretical galaxy formation scenario, there are also approaches which study the history of the mass growth for bound objects and the characteristic times (e.g. Lacey &

Silk 1991; Kauffmann, White & Guiderdoni 1993; Cole et al. 1994). Most of them were based on the extended PS formalism, which was proposed by Bower (1991) and Bond et al. (1991). It can derive the number density of objects of a certain mass at a given time subject to a larger object at a later time. Using the formalism, Lacey & Cole (1993; LC) calculated the “merger” rate.

The PS formalism, however, has a limitation for describing the history of the mass growth about the individual objects. The “merging process” described with the PS approach in LC, cannot be interpreted as the same meaning of the merger in astronomical sense, in which the objects lose their identity. In the mass growth history for the astronomical objects, the continuous accretion onto a bound object without the loss of identity has different meanings from the mass accumulation with the loss of the identity in the major merger. The formalism based with the PS approach can-

arXiv:astro-ph/9910033v1 2 Oct 1999

not imply the distinction between “tiny” and “notable” captures. For solving this problem, Manrique & Salvador-Sole (1995, 1996) proposed a formalism named “ConflUent System of Peak trajectories” (CUSP) formalism as an extension of adaptive windowing by Appel and Jones (1990). They can be categorized into a type of “peak” theory (Doroshkevich 1970; Adler 1981; Bardeen et al. 1986, hereafter BBKS), which can count the number of the peaks of the density related to the collapsing threshold, applying a low-pass filter of the bound object scale to the fluctuation field. The CUSP formalism, unfortunately, needs the iterative calculation to estimate the destruction and the reformation rates with mergers. This point becomes a disadvantage when we try to apply this scheme to the semi-analytical studies for the galaxy formation, including the mass accumulation history of bound objects with Monte Carlo method as shown in LC.

In order to give analytical description for the destruction and the reformation rate in the merger, we developed a new approach called *the skeleton tree formalism*, using the topological characteristics in the smoothing of the random field with Gaussian filter. With the appearance of *sloping saddles* in the landscape of the smoothed field, we can pick up the merging events, and distinguish the merger and the accretion. The topological feature in the landscape with the sloping saddles can be extremely reduced into *skeleton trees*.

In this paper, we will focus on the concept and the basic description of *the skeleton tree formalism*. The outline of the paper is as follows. In Section 2, in order to distinguish the accretion and the merging in our context, we sketch the topological characteristics in the landscape of the smoothed field with critical points; the peaks and the sloping saddles, define the merger events with appearance of the sloping saddles, and reconstruct the growth history of the objects with *skeleton tree* picture. In Sections 3, 4, and 5, we formulate the mathematical description of the constraints, the probability distribution functions, and the scale functions for the critical points. In Section 6, we show the results of the evolution rates with the accretion and the merging obtained from *the skeleton tree formalism* with its consistency. Finally, we present our conclusion in Section 7. We have relegated the details of the derivations to five appendices.

2 IDENTIFICATION OF ACCRETION AND MERGING

2.1 Hierarchical Evolution from Fluctuations and Filtering Process

We will express the density fluctuation field as the functions of the comoving spatial coordinate \mathbf{r} and \mathbf{k} ;

$$\delta(\mathbf{r}) = \int d^3\mathbf{k} e^{i\mathbf{k}\cdot\mathbf{r}} \delta(\mathbf{k}) . \quad (1)$$

Interested collapse objects of a comoving scale R can be identified as peaks greater than a threshold, whose fields are smoothed with a low-pass filter of the resolution scale R . The fluctuation, smoothed with the selection function $S(\mathbf{r}; R)$, can be expressed as

$$F(\mathbf{r}; R) = \frac{\int d^3\mathbf{r}_0 S(\mathbf{r}_0; R) \delta(\mathbf{r} - \mathbf{r}_0)}{\int d^3\mathbf{r}_0 S(\mathbf{r}_0; R)} . \quad (2)$$

This Fourier transform is represented with the window function which is the Fourier transforms of the selection function;

$$F(\mathbf{k}; R) = \delta(\mathbf{k}) W(\mathbf{k}; R) . \quad (3)$$

In our interest cases, the window function works as a low-pass filter.

We shall restrict ourselves to isotropic homogeneous Gaussian random fields with zero mean as descriptions of the initial fluctuations. For the field, the power spectrum is then only a function of $k = |\mathbf{k}|$; $|\delta_{\mathbf{k}}|^2 = |\delta(\mathbf{k})|^2$. The fluctuation spectrum filtered with the scale R is

$$P(k; R) = |\delta_{\mathbf{k}}|^2 W(k; R)^2 . \quad (4)$$

In this paper, we take a normalized isotropic Gaussian filter:

$$W(\mathbf{k}; R) = W(k; R) \equiv e^{-k^2 R^2/2} . \quad (5)$$

In the next subsection, we will discuss the reason related to its unique property for the smoothing.

In the linear theory of gravitational instability for the structure formation, the amplitude of the field in the overdensity area firstly grows in proportion to $D(t)$, where $D(t)$ is the linear growth factor. According to BBKS, a bound object collapses from the area of a comoving scale R when the density of a peak in the fluctuation smoothed over the resolution scale R exceeds above a fixed threshold $\delta_{c;0}$. Instead of viewing the peaks to be growing in density amplitude relative to the fixed threshold $\delta_{c;0}$, we can interpret that the threshold level δ_c is decreasing as $\delta_{c;0} D(t_0) D(t)^{-1}$ with fixing the initial fluctuation field $F(\mathbf{r}; R)$, where $\delta_{c;0}$ was determined from the threshold at the present time t_0 . In this paper, we take Einstein-de Sitter model: $\Omega_0 = 1, \lambda_0 = 0$, in which the relative threshold level $\delta_c/\delta_{c;0} = D(t_0) D(t)^{-1} = (1+z)$, where z is the redshift at the time t .

For standard initial fluctuations like CDM models, in general, the rms of the smoothed field $\langle F(\mathbf{r}; R)^2 \rangle$ is decreasing as increasing R . For such a fluctuation, as decreasing the collapse threshold with time evolution, we can pick the collapse objects in the larger scale, which gives a reasonable sketch of hierarchical clustering picture. We will relate the filtering process and the hierarchical clustering description in the next.

2.2 Landscape of the Fluctuation Field in Position and Resolution Space

Consider the random field in one dimensional (1-D) positional coordinate of x is smoothed with a low-pass filter of a resolution scale R . This field is reproduced as a landscape which extends in two dimensional (2-D) extended space of (x, R) . A smoothing peak with a low-pass filter make a ridge which is running along the direction of increasing R in the landscape. The threshold level of the collapse can be interpreted as an ocean surface which makes a “shoreline” and some “lakes” and “islands” in the landscape. A “cape” on the shoreline of δ_c , can be identified as a bound object at δ_c . Then, we can count the number of the bound objects of the scale R to pick up the capes at the R in the landscape. As the level of the ocean surface of δ_c is decreasing with the evolution of the universe, the shoreline moves to the offing. It means that the bound objects grow their scale continuously.

However, if “islands” or “lakes” appear in the landscape, they confuse the identification of “capes” as bound objects. As an example, let consider an island in the offing of a cape on a shoreline. In this case, we have also another offing side cape of the island; there are two capes which can be counted as the bound objects of “clouds”. In these situations, the cloud of the island cape contains the smaller cloud of the cape on the shore. These problems appear when we take general filters except the Gaussian filter. Bond et al. (1991) had shown the filter dependency of the landscape (see their Figure 1 and 2), in which they take sharp k -space filter and Gaussian filter. In the case of the sharp k -space filter, the ridges cannot decrease monotonically as the resolution scale R increases. On the other hand, in the case of the Gaussian filter, the ridge decreases monotonically as the resolution scale R increases. They represent about this feature as there is no “lake” of finite extent, and the ocean shoreline have no bays. Another property of the Gaussian filtering is that the variance is also monotonically decreasing as increasing R . In general, this picture is also valid in 3-D random field. With the help of this feature, we can distinguish the accretion and the merge in the landscape produced from initial fluctuation fields.

2.3 Definition of Monotonic Accretion and Merging in the Landscape

In order to understand the monotonic evolution of the field smoothed with the Gaussian filter of the resolution scale R , we rewrite the derivative of the field as

$$\frac{\partial F(\mathbf{r}; R)}{\partial R} = R \nabla^2 F(\mathbf{r}; R). \quad (6)$$

This is identical to a diffusion equation of the variables (R^2, \mathbf{r}) . For all critical points of $\nabla^2 F < 0$ ($\nabla^2 F > 0$) like peaks (holes), it guarantees the monotonically decreasing (increasing) as the scale increasing as

$$\frac{\partial F(\mathbf{r}; R)}{\partial R} < 0, \left(\frac{\partial F(\mathbf{r}; R)}{\partial R} > 0 \right). \quad (7)$$

This monotonicity of the peak smoothing also guarantees that the peak runs continuously on the ridge to the shore cape without the island in the landscape. It can be reasonable that the smoothing and the merging of peaks are defined as the continuous accretion growth and the merging event of bound objects. If we have islands in the landscape with other filters of Gaussian, however, we cannot distinguish the accretion and the merging with the confusion for the scale identification of the related bound objects. Fortunately, we can exclude this problem as long as using the Gaussian filter which guarantees the absence of island in the landscape as shown above. This is the reason that we take the Gaussian filter in this paper.

A ridge in the landscape, then, represents continuous accretion growth of a bound object. On the other hand, some ridges terminate on the slope of neighboring ridges. The vanishing point of the ridge on the slope of the neighboring ridge can be defined as a type of critical points. We call it as *sloping saddle* since it is a saddle point on the slope of the neighbor peak. The sloping saddle can represent the reasonable feature that a bound object loses the identity loss in the merger, associated with a tree structure in

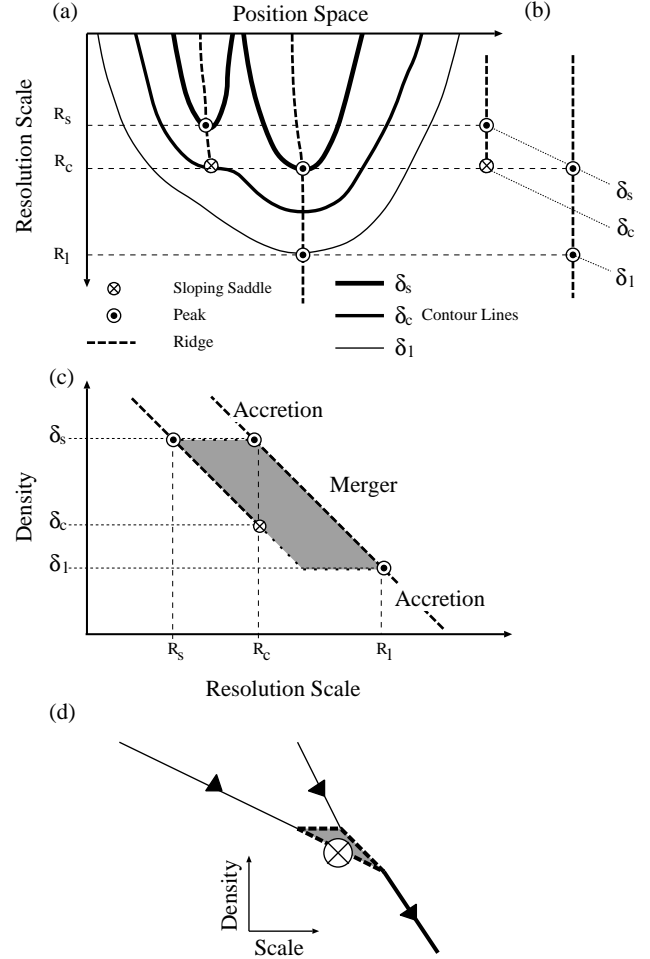


Figure 1. The schematic presentation for the abstraction steps from the smoothing fluctuation field to the *skeleton tree* picture. (a) Schematic representation of the landscape. The symbols of \odot and \otimes means the peak and the sloping saddle, respectively. The peak trajectory with filter smoothing makes the ridge. A ridge terminates at a sloping saddle at (R_c, δ_c) which is associated with a ridge of the neighboring peak through the resolution scale interval from R_c to R_l . (b) The critical points and the ridges are picked up as the abstract tree of the field around a sloping saddle. (c) The tree is presented by the reordering in (R, δ) space. The hatched area means the merger. (d) The graphical presentation of the smoothing peaks with the merger and the accretion in the *skeleton tree formalism*.

which the branches of the ridges are nested at the junctions of the sloping saddles. Then, we can translate the topology in the landscape to the tree structure named with *skeleton tree*, which consists of the accretion branches and the merger junction picked up with the sloping saddles.

2.4 Skeleton Tree Picture

We will describe the abstraction from the landscape to the tree structure as presented in Fig. 1 schematically. In Fig. 1 (a), the local structure of the landscape is represented with contour lines, and the different classes of interest critical

points are marked; the peak as \odot and the sloping saddle as \otimes , and the ridges are represented as the dashed lines. In this example, the sloping saddle appears on a resolution scale R_c at a threshold δ_c . A ridge terminates at the sloping saddle $\otimes(R_c, \delta_c)$. It means that a bound object of the scale R_c loses its identity at the threshold δ_c . There is a ridge neighboring with the sloping saddle, on which the peak has the density of δ_s at the same resolution scale of $\otimes(R_c, \delta_c)$. The peak on the neighboring ridge is reforming around the sloping saddle. Then, we can consider that the reformation starts from (R_c, δ_s) of a peak neighboring with the sloping saddle. The merger with the destruction and the reformation starts from δ_s and ends at δ_l with the scale range from R_s to R_l in the case of Fig. 1 (a).

As shown in Fig. 1 (b) as an abstraction of Fig. 1 (a), then, we can introduce a tree structure associated with the sloping saddle $\otimes(R_c, \delta_c)$ and three peaks; the neighboring peak $\odot(R_c, \delta_s)$ of $\otimes(R_c, \delta_c)$ in the same resolution R_c , the progenitor peak $\odot(R_s, \delta_s)$ on the same ridge of $\otimes(R_c, \delta_c)$ at δ_s of the density of $\odot(R_c, \delta_s)$, and the reformed peak $\odot(R_l, \delta_l)$ on the same ridge of the neighboring $\odot(R_c, \delta_s)$.

For describing the history of the hierarchical clustering with the merging, it is convenient to reorder the tree structure along the threshold level instead with the filtering scale. Because the threshold level is identical to the time as monotonically mapped with $\delta_c = \delta_{c;0}D(t)^{-1}$. Fig. 1 (c) schematically shows this reconstructed feature from the Fig. 1 (b). The continuous accretion growth is represented as the dashed lines along the ridges, while the merger is represented as the hatched area in Fig. 1 (c). In this case, the merger occurs during the interval between δ_l and δ_s . Even if we can follow the neighboring peak on the same ridge over δ_c in the landscape, however, we have two peaks at a threshold during the merger after the reordering with the threshold, as shown in the hatched area in Fig 1. (c). It means that the reforming peak on the ridge neighboring with the sloping saddle also loses its identity with the merger. Then, the neighboring ridge is divided into two part of a disappearing peak $> \delta_c$ and a reforming peak $< \delta_c$.

The merger feature is simplified as a joint, which connects three lines of two disappearing peaks and the reforming peak at a point of the sloping saddle as shown in Fig. 1 (d), where the lines are the abstraction of the ridges as the continuous accretion growth. In the Figure, the line processes of the accretion branches are connected with the point process of the merger at the (R_c, δ_c) , which makes a *skeleton tree*.

In the derivation of the *skeleton tree*, we have neglected the detail features of three peaks around $\otimes(R_c, \delta_c)$ except counting the number of the associated lines, and approximated as the destruction and the reformation occur at (δ_c, R_c) instantaneously. This is reasonable since no other parameter sets except (δ_c, R_c) can be defined without any extra parameter for modeling the merger event. The consistency of this simple picture can be proved with the result in the section 6.

We can practically reproduce accretion and merging with the script of *skeleton tree* as shown in in Fig 1(d); the arrowed line is related to the mass growth with continuous accretion, and the joint of hatching triangle is a merger event with the destruction and the reformation with the mark \otimes of the sloping saddle. We note that the branching number

at the merging points is always two in the progenitor side. This is natural since the merger rate of three or more multi peaks are negligible to that of double peaks.

3 THE CONSTRAINTS OF CRITICAL POINTS

3.1 Line and Point Processes in the Skeleton Tree

As shown in the previous section, *the skeleton tree formalism* is described by a set of the line and point processes of the smoothing peak along the ridge and the sloping saddle in the extended space (\mathbf{r}, R) . The line process of the smoothing peaks in (\mathbf{r}, R) is equal to the point process in the original spatial coordinate \mathbf{r} .

Their density fields of these point processes are described as sums of δ functions :

$$n_{pk}(\mathbf{r}; R) = \sum_i \delta^{(3)}(\mathbf{r} - \mathbf{r}_{pk,i}), \quad (8)$$

$$\mathbf{n}_{ss}(\mathbf{r}, R) = \sum_i \delta^{(3)}(\mathbf{r} - \mathbf{r}_{ss,i})\delta(R - R_{ss,i}), \quad (9)$$

where the subscripts of *pk* and *ss* means peaks and sloping saddles, R_{ss} is the resolution scale of the sloping saddles. Since $n_{pk}d^3\mathbf{r}$ and $\mathbf{n}_{ss}d^3\mathbf{r}dR$ are the numbers in 3-D infinite volume of $d^3\mathbf{r}$ and 4-D infinite volume of $d^3\mathbf{r}dR$, we call the former and the later as the spatial density and the instantaneous spatial density, respectively.

We can express the point processes entirely in terms of the field and its derivatives with the spatial coordinate \mathbf{r} and the resolution scale R . In the neighborhood around a critical point, with its constraint of $\nabla F(\mathbf{r})|_{cr} = 0$, we can expand the field in a Taylor series:

$$F(\mathbf{r}) \simeq F(\mathbf{r}_{cr}) + \frac{1}{2!}\nabla \otimes \nabla F|_{cr}\Delta\mathbf{r}\Delta\mathbf{r} + \frac{1}{3!}\nabla \otimes \nabla \otimes \nabla F|_{cr}\Delta\mathbf{r}\Delta\mathbf{r}\Delta\mathbf{r}, \quad (10)$$

and its derivatives can be also expanded as

$$\nabla F(\mathbf{r}) \simeq \nabla \otimes \nabla F|_{cr}\Delta\mathbf{r}, \quad (11)$$

$$\nabla \otimes \nabla F(\mathbf{r}) \simeq \nabla \otimes \nabla F(\mathbf{r})|_{cr} + \nabla \otimes \nabla \otimes \nabla F|_{cr}\Delta\mathbf{r}, \quad (12)$$

where $\Delta\mathbf{r} = \mathbf{r} - \mathbf{r}_{cr}$ and the suffix *cr* means the value at the critical point.

The critical points can be divided into non-degenerate one and degenerate one. The extrema like a peak and hole can be categorized into non-degenerate one. Provided the condition of the non-degenerate extrema $\det(\nabla \otimes \nabla F)|_{cr} \neq 0$, Eq. (11) can be rewritten to

$$\mathbf{r} - \mathbf{r}_{cr} = (\nabla \otimes \nabla F|_{cr})^{-1}\nabla F(\mathbf{r}). \quad (13)$$

Using the second derivatives of the field, the number density of the extrema can be represented as

$$n_{ex} = \delta^{(3)}((\nabla \otimes \nabla F)^{-1}\nabla F) = |\det(\nabla \otimes \nabla F)|\delta^{(3)}(\nabla F). \quad (14)$$

In order to describe the point process for the extrema, thus, it is enough to take the terms to the order of the second derivatives.

In the degenerate case of $\nabla \otimes \nabla F|_{cr} = 0$, however, we cannot describe the displacement vector only with the first and second derivatives of the field as the non-degenerate case

of Eq. (13). The sloping saddle is a kind of the degenerate critical points.

Under the transformation of the principal axis in the spatial coordinate, the part of six components related to the second derivatives $\nabla \otimes \nabla F$ in the covariance matrix becomes diagonal. It means that the second derivatives have three eigenvalues as

$$(F_{11}, F_{22}, F_{33}) = -\sigma_2(\lambda_1, \lambda_2, \lambda_3), F_{\alpha\beta} = 0 \ (\beta \neq \alpha), \quad (15)$$

where σ_2 is the rms of $\nabla \otimes \nabla F$ (see the definition in Appendix A). All the eigenvalues are not null in the non-degenerate cases. On the other hand, the degenerate critical points has one null eigenvalue at least as $\lambda_3 = 0$, where we assumed $\lambda_1 \geq \lambda_2 \geq \lambda_3$ for convenience. This is the reason for the break of the non-degenerate condition as $\det \nabla \otimes \nabla F|_{cr} = 0$ in the degenerate case. In general, a sloping saddle has a neighboring peak at the degenerate direction. In this degenerate direction, we cannot take the inversion of Eq. (11) as $x_3 - x_{3,cr} = F_{33}|_{cr}^{-1} F_3$ since $F_{33}|_{cr} = 0$.

In order to describe the point process of the sloping saddles, we use the expansions of F_{33} at the degenerate direction and $\nabla^{(2)} F$ for the rest 2-D non-degenerate components in a couple of Eq. (12) and Eq. (11) as

$$F_{33} \simeq \sum_{\beta=1}^3 F_{33\beta} \Delta x_\beta \simeq F_{333} \Delta x_3, \quad (16)$$

$$\nabla^{(2)} F \simeq \nabla^{(2)} \otimes \nabla^{(2)} F \Delta \mathbf{r}^{(2)}, \quad (17)$$

where the suffice of (2) means the 2-D non-degenerate space. The set of the expansions derives

$$\mathbf{r}^{(2)} - \mathbf{r}_{cr}^{(2)} = (\nabla^{(2)} \otimes \nabla^{(2)} F|_{cr})^{-1} \nabla^{(2)} F(\mathbf{r}), \quad (18)$$

$$x_3 - x_{3,ss} = F_{333}^{-1} F_{33}. \quad (19)$$

Furthermore, we should remember that the sloping saddle is defined in the extended space with the resolution scale R . The gradient $\nabla F(\mathbf{r})$ can be expanded with the derivative of R ;

$$\nabla F(\mathbf{r}) \simeq \frac{d\nabla F}{dR}|_{ss} (R - R_{ss}) = \nabla^2 \nabla F|_{ss} R (R - R_{ss}). \quad (20)$$

In the degenerate direction, this gives

$$R - R_{ss} = \left(\sum_{\alpha=1}^3 F_{3\alpha\alpha} R \right)^{-1} F_3. \quad (21)$$

We obtain the constraint for the instantaneous spatial density of the sloping saddles as

$$\begin{aligned} \mathbf{n}_{ss} &= \sum_i \delta^{(3)}(\mathbf{r} - \mathbf{r}_{ss,i}) \delta(R - R_{ss,i}) \\ &= |\det(\nabla^{(2)} \otimes \nabla^{(2)} F)| \delta^{(2)}(\nabla^{(2)} F) \\ &\quad \times |F_{333}| \delta(F_{33}) \left| \sum_{\alpha=1}^3 F_{3\alpha\alpha} R \right| \delta(F_3). \end{aligned} \quad (22)$$

3.2 Constraints of Peaks and Sloping Saddles

Under the transformation to the diagonal principal axis, the peaks require the condition of $\lambda_1 \geq \lambda_2 \geq \lambda_3 \geq 0$ which should be added to the above condition of the extrema: Eq.

(14). With the additional condition of the peaks, the constraint for the spatial distributions of the peaks is

$$C(\mathbf{F}^{(10)} | \text{peaks}) = \sigma_2^3 |\lambda_1 \lambda_2 \lambda_3| \prod_{i=1}^3 \delta(F_\alpha) \prod_{\alpha=1}^3 \theta(\lambda_i), \quad (23)$$

where $\theta(\lambda_i)$ is the Heaviside function.

The sloping saddles requires the additional condition of $\lambda_i > 0$ ($i = 1, 2$) as excluding the merger of the hole. With the constraint of Eq. (22), the constraint for the instantaneous spatial distribution of the sloping saddle can be described as

$$\begin{aligned} C(\mathbf{F}^{(20)} | \text{s.saddles}) &= \sigma_2^2 \sigma_3^2 R |\lambda_1 \lambda_2 w_3 (w_1 + w_2 + w_3)| \\ &\quad \times \delta(\lambda_3) \prod_{\alpha=1}^3 \delta(F_\alpha) \prod_{i=1}^2 \theta(\lambda_i), \end{aligned} \quad (24)$$

where we use $\sigma_3 w_\alpha = F_{3\alpha\alpha}$.

4 PROBABILITY DISTRIBUTION FUNCTION

The joint probability distribution of n-dimensional random variables with multivariate Gaussian can be described as

$$P(\mathbf{F}^{(n)}) d\mathbf{F}^{(n)} = \frac{\exp[\frac{1}{2} \mathbf{F}^{(n)T} \mathbf{C}^{(n \times n)-1} \mathbf{F}^{(n)}]}{(2\pi)^n |\det \mathbf{C}^{(n)}|^{1/2}} d\mathbf{F}^{(n)}. \quad (25)$$

The covariance matrix $\mathbf{C}^{(n \times n)}$ is defined as the expectation value of the direct product of the vector $\mathbf{F}^{(n)}$:

$$C_{\alpha\beta}^{(n \times n)} = \langle F_\alpha^{(n)} F_\beta^{(n)} \rangle, \quad (26)$$

where the suffix (n) of the $\mathbf{F}^{(n)}$ is the dimension of the parameter space.

In general, the conditional probability of the event A with the constraint event B is given by the Bayes formula $P(A|B) = P(A, B)/P(B)$. The joint probability, then, can be expanded with the conditional probabilities. If the parameters in the vector are all Gaussian distributed, we can directly obtain the covariance matrix of the conditional probability. There is a general theorem which is extremely useful when we calculate the above joint probability from the conditional probabilities. For the count of the peaks, we need only the 10 dimension parameters $\mathbf{F}^{(10)} = (F, \nabla F, \nabla \otimes \nabla F)$. For the count of the sloping saddles, we should extend the parameter space to the 20 dimension $\mathbf{F}^{(20)} = (F, \nabla F, \nabla \otimes \nabla F, \nabla \otimes \nabla \otimes \nabla F)$. The 20 dimension covariance matrix can be found with the explicit forms of the parameters in Appendix A. With the help of the theorem (see Appendix B1), the divided conditional probabilities are described for the case of the peaks and the sloping saddles in Appendix B2 and B3, respectively.

For a type of critical points in a n-dimensional parameter space described with constraints, in general, the probability weighted density is

$$n_{cr}(\mathbf{F}^{(n)}) d\mathbf{F}^{(n)} = P(\mathbf{F}^{(n)}) C(\mathbf{F}^{(n)} | \text{cr. points}) d\mathbf{F}^{(n)}. \quad (27)$$

Then, the ensemble averaged density of the type of critical points restricted with m-dimension parameters, can be obtained from the integration over (n-m) dimension parameters;

$$\langle n_{cr}(\mathbf{F}^{(m)}) \rangle d\mathbf{F}^{(m)} = \int d\mathbf{F}^{(n-m)} n_{cr}(\mathbf{F}^{(n)}) d\mathbf{F}^{(m)}. \quad (28)$$

The ensemble averaged density gives the scale function we interest.

5 SCALE FUNCTIONS OF CRITICAL POINTS

We will derive the differential number densities of all the peaks, the nesting peaks, the non-nesting peaks, and the instantaneous differential number density of the sloping saddles, which are presented as the scale functions and the instantaneous scale function of $N_{pk}(R, \delta)dR$, $N_{nest}(R, \delta)dR$, $N_{pk}(R, \delta)dR$, and $\mathbf{N}_{ss}(R, \delta)dRd\delta$, respectively.

The scale functions for all the peaks, the non-nesting, and nesting peaks are briefly given in the appendix C1, C2, and C3, according to BBKS and the CUSP formalism. We had checked that the contribution of the nesting peaks is negligible as shown in Fig. 2. Thus, we treat the scale function of peaks as that of the non-nesting peaks hereafter.

In the first subsection, then, we sketch the derivations of the scale functions of peaks. In the next subsection, we present the new calculation for the instantaneous scale function for the sloping saddles.

5.1 Scale Function of Peaks

The scale function of $N_{pk}(R, \delta)dR$ can be calculated from the ensemble-averaged density of the peak $\mathcal{N}_{pk}(\nu; R)d\nu = \langle n_{pk}(\nu; R) \rangle d\nu$, where $\nu = \delta/\sigma_0$, according to Manrique & Salvador-Sole (1995). The scale function means the differential number density per infinitesimal range of R at a fixed ν , not from that per infinitesimal range of ν at a fixed R . The forward one and the last one are denoted by a roman capital and a caligraphic capital which is the same as the notation of BBKS, respectively. The spatial density for the peaks of the non-degenerate critical points with a certain filtering scale can be calculated by the same way of BBKS.

In order to obtain the density of peaks with up-crossing a certain δ_c in the range of the filtering scale between $R - \Delta R$ and R , we should pick up the critical points which are equal to or smaller than δ_c at the filtering scale of R and becomes larger than δ_c at the smaller filtering scale of $R - \Delta R$. It means that we should count the peaks of $\delta_c + (dF_{pk}/dR)\Delta R < F_{pk} < \delta_c$ on scale R . As shown in the discussion of the Gaussian filtering, the condition of the counting is expressed as

$$\delta_c + \nabla^2 F R \Delta R < F < \delta_c. \quad (29)$$

As obtained for the peaks in BBKS, in general, we can obtain the spatial number density of the peaks in infinite ranges $d\nu dx$ of the density contrast ν and the second derivative of it with a certain filtering scale R ; $\mathcal{N}_{pk}(\nu, x; R)d\nu dx$. We can transform this number density to the number satisfying the condition of the our counting;

$$\begin{aligned} N_{pk}(R, \delta_c) &= \lim_{\Delta R \rightarrow 0} \frac{1}{\Delta R} \int_0^\infty dx \int_{\nu_{c,b}}^{\nu_c} d\nu \mathcal{N}_{pk}(\nu, x; R) \\ &= \mathcal{N}_{pk}(\nu_c; R) \langle x \rangle_{pk} \left(\frac{\sigma_2(R)}{\sigma_0(R)} \right) R, \end{aligned} \quad (30)$$

$$\nu_{c,b} = \nu_c - x \left(\frac{\sigma_2(R)}{\sigma_0(R)} \right) R \Delta R, \quad (31)$$

where $\langle x \rangle_{pk}$ is the mean value of x defined from the distribution function as

$$\langle x \rangle_{pk} = \frac{H_{pk}(\gamma, \gamma\nu_c)}{G_{pk}(\gamma, \gamma\nu_c)}, \quad (32)$$

In practical treatment, we can use the averaged mapping relation

$$d\nu_c \simeq \langle x \rangle_{pk} \left(\frac{\sigma_2(R)}{\sigma_0(R)} \right) R dR. \quad (33)$$

Fig. 2 illustrates $N_{pk}(R, \delta_c)RR_0^2$ and $N^{nest}(R, \delta_c)RR_0^2$ versus R/R_0 with the present collapsing threshold condition $\delta_c = 1.68$ in the power-law fluctuations of $n = 0, -1$, and -2 . The former and the latter are represented with the solid and dotted lines, respectively. The critical scale of R_0 , was determined by $\delta_c/\sigma_0(R_0) = 1$ with $\delta_c = 1.68$. The number of the nesting peaks is negligible compared with that of all peaks. Hereafter, then, we will take $N(R, \delta_c) = N_{pk}(R, \delta_c)$. The PS scale functions, obtained from the same filtered random fields, are also presented with the dashed lines. We also present the two scale functions of peaks for standard CDM (SCDM) model with the normalization of 8 Mpc with the bias factor $b = 1$. Even if the two functions in the small scale are different from each other between the peak theory and the PS formalism as pointed out by Appel & Jones (1991), they deviate relatively little over the cosmological interest interval (2 decades in the filter scale, 6 decades in the mass scale around R_0).

Fig. 2 shows that the scale functions of the peaks $N_{pk}(R, \delta_c)RR_0^2$ become proportional to R^{-3} asymptotically in the small scale. As shown in BBKS, the cumulative number is a useful quantity which can be evaluated analytically:

$$n_{pk}(\nu_c = -\infty) = \int_{\nu_c = -\infty}^{\infty} \mathcal{N}_{pk} d\nu = \frac{29 - 6\sqrt{6}}{5^{3/2} 2(2\pi)^2} R_*^{-3}, \quad (34)$$

As $R \rightarrow 0$, the density contrast $\nu_c \rightarrow 0$ and the peaks of the low contrast ν_c dominates in the cumulative number. Then, $N_{pk}(R, \delta_c)RR_0^2 \propto n_{pk}(\nu_c \rightarrow 0; R_*) \propto n_{pk}(\nu_c = -\infty; R_*)$ in the small scale. Since R_* is proportional to the resolution scale R , the asymptotic feature seen in Fig. 2 is not unexpected thing.

5.2 Instantaneous Scale Function of Sloping Saddles

The instantaneous scale function of sloping saddles can be directly calculated as its ensemble-averaged density:

$$\mathbf{N}_{ss}(R, \nu_c)dRd\nu_c = \langle \mathbf{n}_{ss}(\nu_c; R) \rangle dRd\nu_c. \quad (35)$$

The brief calculation is described in the appendix C.

We should note that the scale function is defined as the density in the infinite interval $dRd\nu_c$. The scale function of the peaks $N_{pk}(R, \delta_c)dR$ introduced before is the differential density of peaks per infinitesimal ranges of the resolution scale R at a fixed density threshold δ_c . On the other hand, the instantaneous scale function of the sloping saddles $\mathbf{N}_{ss}(R, \delta_c)$ is the differential density per infinitesimal ranges of R and δ . Their difference come from the fact that the point processes of peaks and sloping saddles can be defined in the 3-D spatial coordinate and the 4-D space extended with R , respectively. Then, the instantaneous scale function is responsible for the time evolution properties of the scale

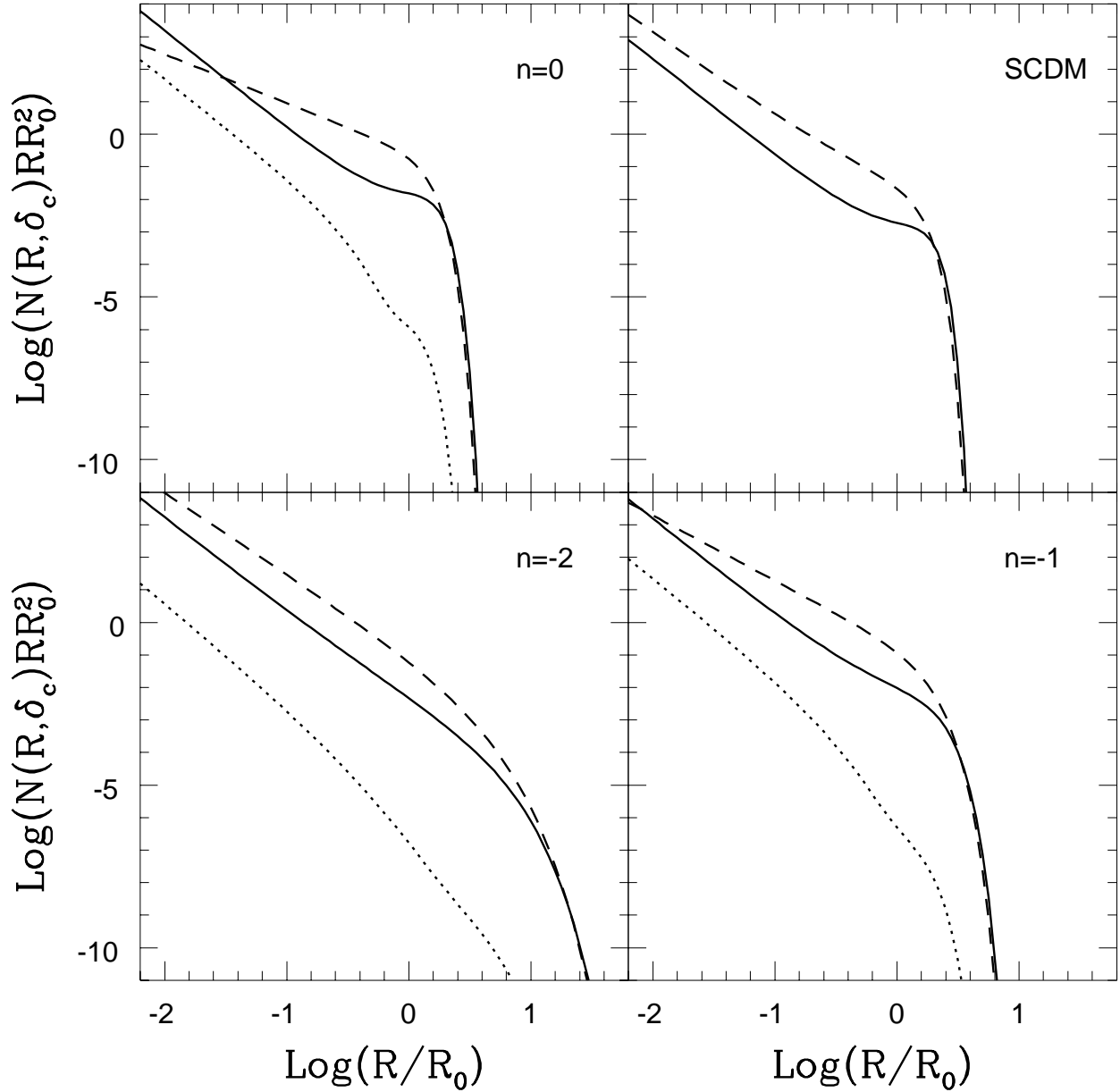


Figure 2. The scale functions are presented for various fluctuation models of the initial density fluctuation. The solid and dotted lines represent the scale function of the all peaks and the nesting peaks. The dashed line is that of the PS formalism with the same filter.

function with the merging process as seen in the *skeleton tree*; the line of the smoothing peak connected with other lines at the junction of the sloping saddle. In the next section, using the *skeleton tree formalism*, we will present the evolution of the scale functions with the distinction between the merger and the accretion according to the *skeleton tree formalism*.

6 EVOLUTION WITH MERGER AND ACCRETION

6.1 Instantaneous Scale Functions for the Disappearing and Reforming Peaks

As discussed in the sketch of the *skeleton tree* picture with Fig. 1, the reformation of a peak can be only identified with the destruction of two peaks around a sloping saddle. In the above section, we can obtain the instantaneous number density of the merger of a scale R at δ_c in the infinite interval

of $d\delta_c$. Thus, with changing between the variables δ_c and ν_c , the instantaneous scale functions of the destruction and the reformation for the peaks of the scale R at δ_c are described as

$$\mathbf{N}^d(R, \delta_c)dR d\delta_c \simeq 2\mathbf{N}_{ss}(R, \delta_c)dR d\nu_c, \quad (36)$$

$$\mathbf{N}^f(R, \delta_c)dR d\delta_c \simeq \mathbf{N}_{ss}(R, \delta_c)dR d\nu_c, \quad (37)$$

where the superscripts of f and d mean the reformation and the destruction in the merger, respectively.

With the formula, the net change of the differential number density of the peaks in dR during the interval of $d\delta_c$ is simplified to

$$\begin{aligned} S(R, \delta_c)dR d\delta_c &= \mathbf{N}^f(R, \delta_c)dR d\delta_c - \mathbf{N}^d(R, \delta_c)dR d\delta_c \\ &= -\mathbf{N}_{ss}(R, \delta_c)dR d\nu_c. \end{aligned} \quad (38)$$

It means the net destruction of the peaks is the same as the appearance of the sloping saddles. This is reasonable since the formation of the peaks does not occur in exact sense and all peaks only disappear at the sloping saddle in the original filtering process. From the concept of the *skeleton tree*, the peak neighboring with a sloping saddle is interpreted to lose its identity with the merger. We considered that the ridge of the neighboring peak is divided into two part of a disappearing peak $> \delta_c$ and a reforming peak $< \delta_c$, even if the ridge of the neighboring peak continues over δ_c . Thus, the reforming number of the peaks can compensate for the destruction of them, and the appearing number of the sloping saddles lefts as the net disappearing number of the peaks. The consistency of this formula can be checked with the conservation equation for the scale function of the peaks, as shown in the next subsection.

6.2 Instantaneous Rates for Accretion, Destruction and Reformation

We will consider the instantaneous scale growth rate for a peak of R as the continuous scale growth of the accretion. The accretion growth rate can be described with the scaled Laplacian x as

$$\dot{R}_{acc}(R, x, \delta_c)dt \equiv \frac{1}{x\sigma_2 R}d\delta_c. \quad (39)$$

We should note that the growth rate for a peak depends on its particular value x . According to Manrique & Salvador-Sole (1996), the mean growth rate for the objects of the scale R can be expressed as

$$\dot{R}_{acc}(R, t)dt \equiv \langle \frac{1}{x\sigma_2 R} \rangle d\delta_c \simeq \frac{1}{\langle x \rangle_{pk} \sigma_2 R}d\delta_c, \quad (40)$$

where $\langle \rangle$ means the average of the function with x and we used the relation

$$\begin{aligned} \langle x^{-1} \rangle &\simeq \frac{\int_0^\infty dx x^{-1} N_{pk}(R, \delta_c, x)dR}{\int_0^\infty dx N_{pk}(R, \delta_c, x)dR} \\ &= \frac{\int_0^\infty dx N_{pk}(\nu_c, x; R) \frac{\sigma_2}{\sigma_0} dR}{\int_0^\infty dx x N_{pk}(\nu_c, x, R) \frac{\sigma_2}{\sigma_0} dR} \\ &= \frac{G_{pk}(\gamma, \gamma\nu_c)}{H_{pk}(\gamma, \gamma\nu_c)} = \langle x \rangle_{pk}^{-1}. \end{aligned} \quad (41)$$

From this mean scale growth rate, we can define the relative growth rate with the accretion as

$$r^a(R, t)dt \equiv \frac{\partial \dot{R}_{acc}(R, t')}{\partial R}. \quad (42)$$

With the similar consideration applied for the merging objects, we can introduce the mean scale growth rate and relative growth rate contributed with continuous accretion during the merger phase;

$$\dot{R}_{acc,m}(R, t)dt \simeq \frac{1}{\langle x \rangle_{ss} \sigma_2 R}d\delta_c, \quad (43)$$

$$r_m^a(R, t)dt \equiv \frac{\partial \dot{R}_{acc,m}(R, t')}{\partial R}, \quad (44)$$

where $\langle x \rangle_{ss} = H_{ss}(\gamma, \kappa, \gamma\nu_c)/G_{ss}(\gamma, \kappa, \gamma\nu_c)$.

The instantaneous destruction and reformation rates can be defined directly from their instantaneous scale functions as

$$r^d(R, t)dt = \frac{\mathbf{N}^d(R, \delta)dR}{N(R, t)dR}d\delta \quad (45)$$

$$r^f(R, t)dt = \frac{\mathbf{N}^f(R, \delta)dR}{N(R, t)dR}d\delta. \quad (46)$$

Thus, the conservation equation for the scale function $N(R, t)$ is given as

$$\frac{\partial N(R, t)}{\partial t} + \frac{\partial (\dot{R}_{acc}N(R, t))}{\partial R} = S(R, t), \quad (47)$$

where $S(R, t)$ can be given as the net source term with the destruction and reformation rates of $r^d(R, t)$ and $r^f(R, t)$;

$$S(R, t) = [r^f(R, t) - r^d(R, t)]N(R, t). \quad (48)$$

The conservation equation can be rewritten to

$$\frac{d \ln N(R, t)}{dt} = r^f(R, t) - r^d(R, t) - r^a(R, t), \quad (49)$$

which can be rewritten to

$$\frac{\partial \ln N(R, t)}{\partial t} = r^s(R, t) + r^f(R, t) - r^d(R, t) - r^a(R, t), \quad (50)$$

where

$$r^s(R, t) = -\dot{R}_{acc} \frac{\partial \ln N(R, t)}{\partial R}, \quad (51)$$

is the rate of shift in the scale space with the accretion for the number density distribution.

The inverses of these rates of $r^{a,f,d,s}(R, t)$ give the time scales of the individual processes. In Fig. 3, the rates for the reformation, the destruction, the relative growth with accretion, the relative growth with continuous accretion for merging objects and the shift in the scale with the accretion at the present are presented with solid, dotted, short dashed, long dashed, and long dash-dotted lines. The left hand side and the right hand side of the conservation equation (52) are also presented with short dash-dotted line and crosses, the former $\partial \ln N(R, t)/\partial t$ can be calculated with the partial time derivative of $N_{pk}(R, t)$ and the latter is calculated from the set of the individual rates as $r^s(R, t) + r^f(R, t) - r^d(R, t) - r^a(R, t)$.

We can see that the partial time derivative of $\partial \ln N(R, t)/\partial t$ can be reproduced well from the right hand side of the conservation equation from the individual calculations of $r^s(R, t)$, $r^f(R, t)$, $r^d(R, t)$, and $r^a(R, t)$ as shown

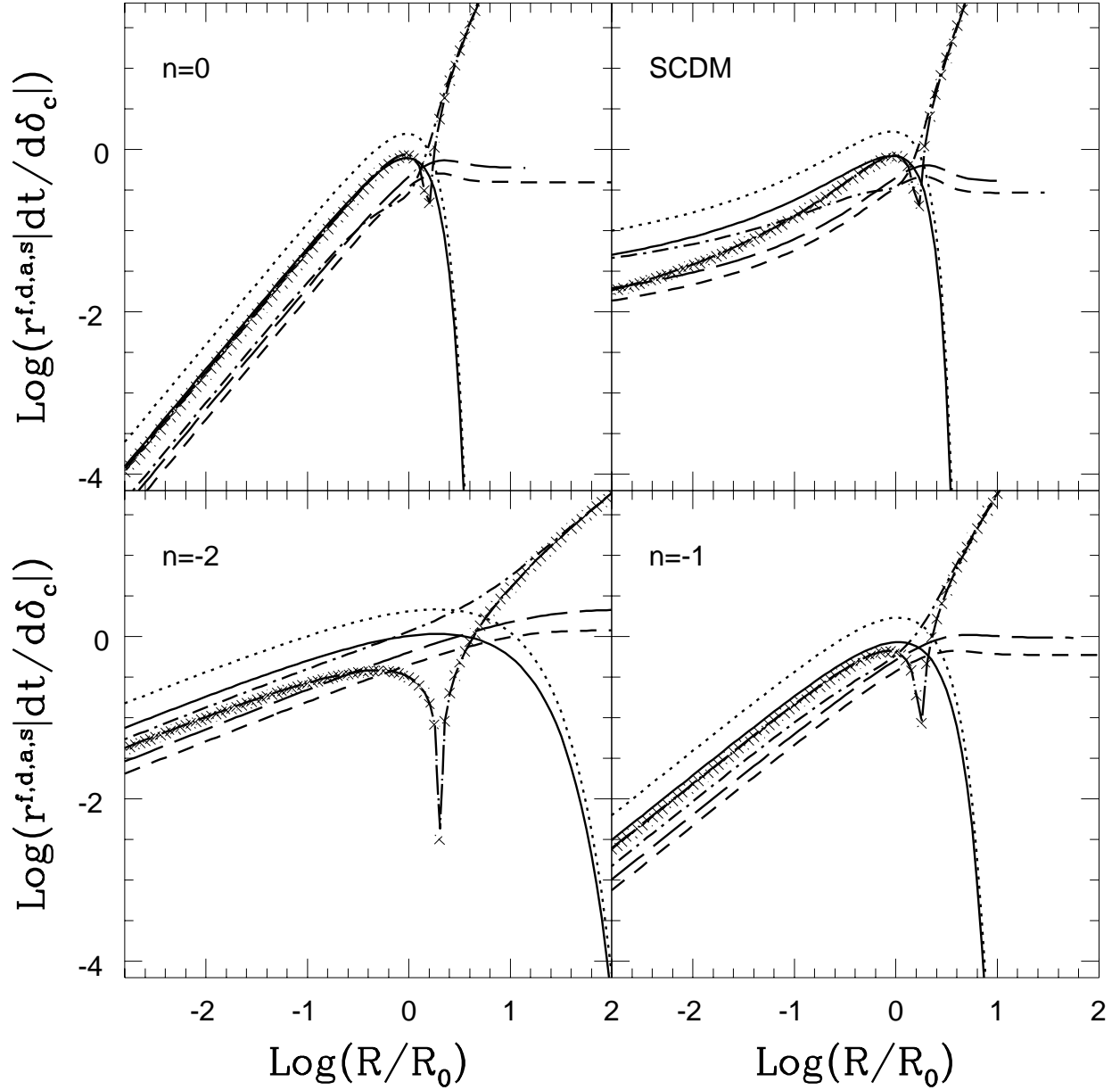


Figure 3. The rates for the evolution processes at the present with $\delta_c = 1.68$. The solid, dotted, short dashed, long dashed, and long dash-dotted lines mean the reformation rate $r^f|dt/d\delta_c|$, the destruction rate $r^d|dt/d\delta_c|$, the relative accretion rate $r^a|dt/d\delta_c|$, the relative accretion rate $r^a|dt/d\delta_c|$ during the merger, and the shift rate $r^s|dt/d\delta_c|$, respectively. The evolution rate of the scale function $|\partial \ln N_{pk}(R, t)/\partial t dt/d\delta_c|$ and the right hand side of the conservation equation (51) is presented by short dash-dotted line and crosses. The absolute values are presented for the two last rates.

in Fig. 3. Especially, around the scale of $R \simeq R_0$, both of them shows the same feature, in which the values shapely switch from negative to positive. Then, we can verify the consistency of our formalism with the equality between the

left hand side and the right hand side of the conservation equation.

The rates of the reformation and the destruction have a maximum around $R \simeq R_0$ and rapidly decrease for the larger scale. On the other hand, the accretion dominates

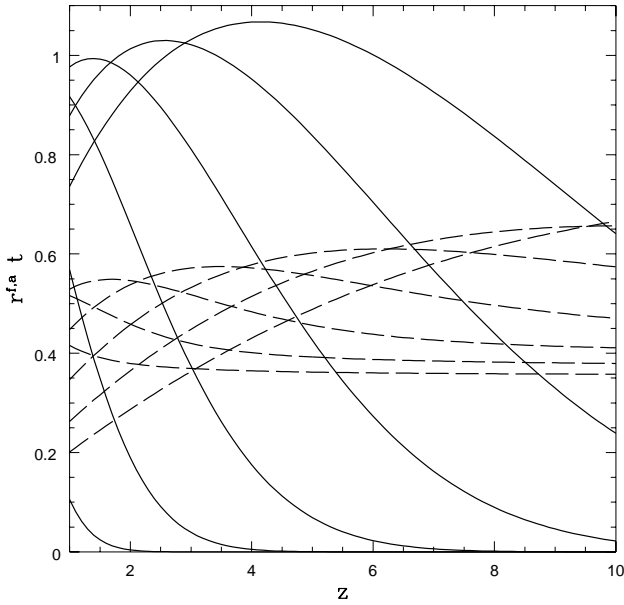


Figure 4. The evolution of growth rates at fixed masses for the SCDM model in an Einstein-de Sitter universe. The solid and dashed lines present the merger and the accretion growth rate $r^f \cdot t$ and $r^a \cdot t$. In the figure, the highest curves at the right is for $M/M_0 = 10^{-2}$, and successive curves are for $M/M_0 = 10^{-1.5}, 10^{-1}, 10^{-0.5}, 1, 10^{0.5}$ and 10^1 .

the merger processes of the reformation and the destruction and the rate becomes almost constant for the large objects ($R \gg R_0$). It is consistent with the picture that the large object are growing in the cosmic time scale. These mean that the larger objects of $R > R_0$ grows with the accretion in the linear regime of the gravitational instability, while the smaller objects are accumulated into the larger objects with the merging in the non-linear gravitational growth regime under the critical scale of R_0 , which is related to the present threshold δ_c . In the theory of gravitational instability, the smaller than R_0 can become in non-linear growth. We should remark that the merger process is the most efficient around the critical scale R_0 even if the merger still dominates the accretion in the small scale. These properties of the dominating merger around R_0 are already suggested from the previous N-body calculations (e.g. Navaro, Frenk, & White 1997).

From the view point of the mass growth history for a object of the scale R , the results in Fig. 3 should indicate that the dominant growth process switches from the accretion to the merger accumulation around the threshold of $\delta = \sigma_0(R)$ and the merger accumulation rate becomes maximum and decreases rapidly. We can see directly this feature in Fig. 4, which represents the evolution of the growth rate with the reformation and the accretion at fixed scales. From these results, in general, the growth of a halo firstly starts with the accretion process, secondly switches to the merging and

is suppressed soon after the merger dominates. This feature also was remarked from the simulations.

We should remark that the results in Fig. 4 are not the mean growth histories for the individual objects since the fixed scales cannot be directly related to the final scales of the objects at the present due to the successive destruction and the reformation cooperated with the accretion. In order to reconstruct the mean growth history for a individual objects, we should extend the basic of *the skeleton tree formalism* including the background effects. This extension of *the skeleton tree formalism* will be described in the following papers.

7 CONCLUSION

We have derived an analytical expression for the statistics and the evolution of the cosmic bound objects with the reformation, the destruction and the accretion. It is applicable to any hierarchical clustering models in which structure grows via gravitational instability. *The skeleton formalism* is derived as a natural expansion of the peaks theory of BBKS. In the landscape reproduced from the random field with the Gaussian filter, we have followed the smoothing of the peaks as the accretion growth of the objects, and have picked up the “sloping saddles” as the merging events with the destruction and the reformation of the objects. The line and point processes of the peaks and sloping saddles in the landscape produce the tree structure. Then, we call our scheme as *the skeleton tree formalism*. With *the skeleton tree formalism*, we can estimate the rates of the reformation, destruction, and the accretion in any hierarchical clustering models. The set of these rates can reproduce the evolution of the scale function of the objects with the conservation equation. This reproduction of the evolving scale function verifies the self-consistency of *the skeleton tree formalism*. With the rate calculation of the individual processes, we can find the merger processes are efficient around the critical scale of R_0 determined as $\delta_c = \sigma_0(R_0)$. The dominant growth process of the objects switches from the accretion to the merger accumulation around the critical threshold related to the scale. It is important to reproduce the mass growth history with distinguish between the accretion and the merger when we try to reproduce the cosmic structure and the galaxy formation in the hierarchical scenario.

ACKNOWLEDGMENTS

The author is grateful to H.J. Mo and S.D.M. White for warm hospitality and the discussions when H. H. visited in MPA in Garching. This works was partially supported by a Grant-in-Aid from Japanese Ministry of Education, Science and Culture.

REFERENCES

- Adler, R.J. 1981, *The Geometry of Random Fields* (Chichester: Wiley)
- Appel, L. & Jones, B.J.T. 1990, MNRAS, 245, 522
- Bardeen, J.M. et al. 1986, ApJ, 304, 15 (BBKS)
- Bond, J.R. et al. 1991, ApJ, 379, 440

Bower, R.J., 1991, MNRAS, 248, 332
 Cole, S. et al. 1994, MNRAS, 271, 781
 Dorshkevich, A.G. 1970, Astrophysica, 6, 30
 Kauffmann, G., White, S.D.M. & Guiderdoni, B. 1993, MNRAS, 264, 201
 Lacey, C. & Cole, S. 1993, MNRAS, 262, 627
 Lacey, C. & Cole, S. 1994, MNRAS, 271, 921
 Manrique, A & Salvador-Sole, E. 1995, ApJ, 433, 6
 Manrique, A & Salvador-Sole, E. 1996, ApJ, 467, 504
 Navarro, J.F., Frenk, C.S. & White, S.D.M. 1997, 490, 493
 Press, W.H. & Schechter, P. 1974, ApJ, 187, 425

APPENDIX A: THE COVARIANCE MATRIX

We will introduce 20-dimension vector $\mathbf{F}^{(20)} = (F, \nabla F, \nabla \otimes \nabla F, \nabla \otimes \nabla \otimes \nabla F, \dots)$. The $\nabla F, \nabla \otimes \nabla F$, and $\nabla \otimes \nabla \otimes \nabla F$ have three, six and ten independent components, respectively. They can be expressed in terms of Fourier transforms:

$$F(\mathbf{r}; R) = \int d^3\mathbf{k} e^{i\mathbf{k}\cdot\mathbf{r}} F(k; R), \quad (\text{A1})$$

$$F_\alpha(\mathbf{r}; R) = \frac{\partial F(\mathbf{r}; R)}{\partial x_\alpha} = i \int d^3\mathbf{k} e^{i\mathbf{k}\cdot\mathbf{r}} k_\alpha F(k; R), \quad (\text{A2})$$

$$\begin{aligned} F_{\alpha\beta}(\mathbf{r}; R) &= \frac{\partial^2 F(\mathbf{r}; R)}{\partial x_\alpha \partial x_\beta} \\ &= - \int d^3\mathbf{k} e^{i\mathbf{k}\cdot\mathbf{r}} k_\alpha k_\beta F(k; R), \end{aligned} \quad (\text{A3})$$

$$\begin{aligned} F_{\alpha\beta\gamma}(\mathbf{r}; R) &= \frac{\partial^3 F(\mathbf{r}; R)}{\partial x_\alpha \partial x_\beta \partial x_\gamma} \\ &= -i \int d^3\mathbf{k} e^{i\mathbf{k}\cdot\mathbf{r}} k_\alpha k_\beta k_\gamma F(k; R). \end{aligned} \quad (\text{A4})$$

It is useful to introduce the integrals over the filtered fluctuation spectrum:

$$\sigma_j^2(R) = 4\pi \int_0^\infty dk k^{2j+2} P(k; R), \quad (\text{A5})$$

when transforming the above values to the non-dimensional ones.

The covariance matrix $\mathbf{C}^{(20)}$ is defined as the expectation value of the direct product of the vector $\mathbf{F}^{(20)}$:

$$C_{ij}^{(20)} = \langle F_i^{(20)} F_j^{(20)} \rangle. \quad (\text{A6})$$

We can represent the matrix as

$$\mathbf{C}^{(20)} = \begin{pmatrix} \sigma_0^2 & \mathbf{0} & \mathbf{M}_{02}^T & \mathbf{0} \\ \mathbf{0} & \mathbf{M}_{11} & \mathbf{0} & \mathbf{M}_{13}^T \\ \mathbf{M}_{02} & \mathbf{0} & \mathbf{M}_{22} & \mathbf{0} \\ \mathbf{0} & \mathbf{M}_{13} & \mathbf{0} & \mathbf{M}_{33} \end{pmatrix}, \quad (\text{A7})$$

$$\mathbf{M}_{11} = \frac{\sigma_1^2}{3} \mathbf{I}^{(3 \times 3)}, \quad (\text{A8})$$

$$\mathbf{M}_{22} = \frac{\sigma_2^2}{5} \overline{\mathbf{M}}_{22}, \quad (\text{A9})$$

$$\overline{\mathbf{M}}_{22} = \begin{pmatrix} 1 & 1/3 & 1/3 & \\ 1/3 & 1 & 1/3 & \mathbf{0} \\ 1/3 & 1/3 & 1 & \\ \mathbf{0} & & & 1/3 \mathbf{I}^{(3 \times 3)} \end{pmatrix}, \quad (\text{A10})$$

$$\mathbf{M}_{33} = \frac{\sigma_3^2}{7} \begin{pmatrix} \overline{\mathbf{M}}_{33} & \mathbf{0} & \mathbf{0} & \mathbf{0} \\ \mathbf{0} & \overline{\mathbf{M}}_{33} & \mathbf{0} & \mathbf{0} \\ \mathbf{0} & \mathbf{0} & \overline{\mathbf{M}}_{33} & \mathbf{0} \\ \mathbf{0} & \mathbf{0} & \mathbf{0} & 1/15 \end{pmatrix}, \quad (\text{A11})$$

$$\overline{\mathbf{M}}_{33} = \begin{pmatrix} 1 & 1/5 & 1/5 \\ 1/5 & 1/5 & 1/15 \\ 1/5 & 1/15 & 1/5 \end{pmatrix}, \quad (\text{A12})$$

$$\mathbf{M}_{02} = -\frac{\sigma_1^2}{3} (\mathbf{K}^{(1 \times 3)}, \mathbf{0}^{(1 \times 3)}), \quad (\text{A13})$$

$$\mathbf{M}_{13} = -\frac{\sigma_2^2}{5} (\overline{\mathbf{M}}_{13}^1, \overline{\mathbf{M}}_{13}^2, \overline{\mathbf{M}}_{13}^3, \mathbf{0}^{(3 \times 1)}), \quad (\text{A14})$$

$$\overline{\mathbf{M}}_{13}^l = \mathbf{e}_l^T \otimes (1, 1/3, 1/3), \quad \mathbf{e}_i = (\delta_{1i}, \delta_{2i}, \delta_{3i}), \quad (\text{A15})$$

where $\mathbf{K}^{(n \times m)}, \mathbf{I}^{(n \times n)}$ and $\mathbf{0}^{(n \times m)}$ is the $(n \times m)$ dimension matrix with every entry unity, the $(n \times n)$ dimension unit matrix and the $(n \times m)$ dimension null matrix, respectively.

APPENDIX B: CALCULATIONS OF JOINT PROBABILITIES

B1 Theorem for the Joint Probability Expansion

According to Adler (1981) and BBKS, all Gaussian distributed parameters represented by the n-dimension vector $\mathbf{Z} = (\mathbf{Y}, \mathbf{X})$, which can be devised into m-dimension vector \mathbf{Y} and (n-m) dimension vector \mathbf{X} , imply us that the conditional probability $P(\mathbf{Y} | \mathbf{X})$ is a Gaussian

$$P(\mathbf{Y} | \mathbf{X}) = \frac{\exp[-\frac{1}{2} \overline{\Delta \mathbf{Y}}^T \langle \overline{\Delta \mathbf{Y}} \otimes \overline{\Delta \mathbf{Y}} | \Delta \mathbf{X} \rangle^{-1} \overline{\Delta \mathbf{Y}}]}{(2\pi)^{m/2} |\det \langle \overline{\Delta \mathbf{Y}} \otimes \overline{\Delta \mathbf{Y}} | \overline{\Delta \mathbf{X}} \rangle|^{1/2}}. \quad (\text{B1})$$

where $\overline{\Delta \mathbf{Y}} = \Delta \mathbf{Y} - \langle \Delta \mathbf{Y} | \Delta \mathbf{X} \rangle$, with the mean;

$$\begin{aligned} \langle \Delta \mathbf{Y} | \Delta \mathbf{X} \rangle &= \langle \Delta \mathbf{Y} \otimes \Delta \mathbf{X} \rangle \langle \Delta \mathbf{X}^2 \rangle^{-1} \Delta \mathbf{X} \\ \langle \Delta \mathbf{X}^2 \rangle^{-1} &= \langle \Delta \mathbf{X} \otimes \Delta \mathbf{X} \rangle^{-1}, \end{aligned} \quad (\text{B2}) \quad (\text{B3})$$

and the conditional covariance matrix:

$$\begin{aligned} \mathbf{C}(\mathbf{Y} | \mathbf{X}) &= \langle \overline{\Delta \mathbf{Y}} \otimes \overline{\Delta \mathbf{Y}} | \Delta \mathbf{X} \rangle \\ &= \langle \Delta \mathbf{Y} \otimes \Delta \mathbf{Y} \rangle \\ &\quad - \langle \Delta \mathbf{Y} \otimes \Delta \mathbf{X} \rangle \langle \Delta \mathbf{X}^2 \rangle^{-1} \langle \Delta \mathbf{X} \otimes \Delta \mathbf{Y} \rangle, \end{aligned} \quad (\text{B4})$$

where $\langle \rangle$ represents the mean value and $\Delta \mathbf{X} = \mathbf{X} - \langle \mathbf{X} \rangle$. With the theorem, we can obtain the conditional probabilities from the covariance matrix.

B2 Divided Conditional Probability

We can expand the joint probability distribution with the conditional probabilities as

$$\begin{aligned} P(F, F_\alpha, F_{\alpha\beta}, F_{\alpha\beta\gamma}) dF dF_\alpha^{(3)} dF_{\alpha\beta}^{(6)} dF_{\alpha\beta\gamma}^{(10)} &= \\ P(F_{\alpha\beta\gamma} | F, F_\alpha, F_{\alpha\beta}) dF_{\alpha\beta\gamma}^{(10)} & \\ \times P(F, F_\alpha, F_{\alpha\beta}) dF dF_\alpha^{(3)} dF_{\alpha\beta}^{(6)} & \quad (\text{B5}) \end{aligned}$$

$$\begin{aligned} P(F, F_\alpha, F_{\alpha\beta}) dF dF_\alpha^{(3)} dF_{\alpha\beta}^{(6)} &= \\ P(F_{\alpha\beta} | F, F_\alpha) dF_{\alpha\beta}^{(6)} P(F, F_\alpha) dF dF_\alpha^{(3)}. & \quad (\text{B6}) \end{aligned}$$

Using the theorem above, these conditional probability functions are represented in the explicit forms:

$$P(F, F_\alpha) = \frac{3^{3/2} \exp[-\frac{1}{2} Q(F, F_\alpha)]}{(2\pi)^2 \sigma_1^3 \sigma_0}, \quad (\text{B7})$$

$$\begin{aligned} P(F_{\alpha\beta} | F, F_\alpha) &= P(F_{\alpha\beta} | F) \\ &= \frac{\exp[-\frac{1}{2} Q(F_{\alpha\beta} | F)]}{(2\pi)^3 |\det \mathbf{C}(F_{\alpha\beta} | F)|^{1/2}}, \end{aligned} \quad (\text{B8})$$

$$\begin{aligned}
P(F_{\alpha\beta\gamma}|F, F_\alpha, F_{\alpha\beta}) &= P(F_{\alpha\beta\gamma}|F_\alpha) \\
&= \frac{\exp[-\frac{1}{2}Q(F_{\alpha\beta\gamma}|F_\alpha)]}{(2\pi)^5 |\det \mathbf{C}(F_{\alpha\beta\gamma}|F_\alpha)|^{1/2}}, \quad (\text{B9})
\end{aligned}$$

where

$$Q(F, F_\alpha) = \frac{F^2}{\sigma_0^2} + \frac{3F_\alpha F_\alpha}{\sigma_1^2}, \quad (\text{B10})$$

$$Q(F_{\alpha\beta}|F) = \tilde{F}_{\alpha\beta}^T \mathbf{C}(F_{\alpha\beta}|F)^{-1} \tilde{F}_{\alpha\beta}, \quad (\text{B11})$$

$$Q(F_{\alpha\beta\gamma}|F_\alpha) = \tilde{F}_{\alpha\beta\gamma}^T \mathbf{C}(F_{\alpha\beta\gamma}|F_\alpha)^{-1} \tilde{F}_{\alpha\beta\gamma}, \quad (\text{B12})$$

$$\tilde{F}_{\alpha\beta} = F_{\alpha\beta} - \mathbf{M}_{02} \sigma_0^{-2} F, \quad (\text{B13})$$

$$\tilde{F}_{\alpha\beta\gamma} = F_{\alpha\beta\gamma} - 3\sigma_1^{-2} \mathbf{M}_{13} F_\alpha, \quad (\text{B14})$$

and the conditional covariance matrix;

$$\begin{aligned}
\mathbf{C}(F_{\alpha\beta}|F) &= \mathbf{M}_{22} - \mathbf{M}_{02}^T \sigma_0^{-2} \mathbf{M}_{02} \\
&= \frac{\sigma_2^2}{5} (\overline{\mathbf{M}}_{22} - \overline{\mathbf{M}}_{202}), \quad (\text{B15})
\end{aligned}$$

$$\overline{\mathbf{M}}_{202} = \frac{5\sigma_1^4}{9\sigma_2^2 \sigma_0^2} \begin{pmatrix} \mathbf{K}^{(3 \times 3)} & \mathbf{0}^{(3 \times 3)} \\ \mathbf{0}^{(3 \times 3)} & \mathbf{0}^{(3 \times 3)} \end{pmatrix}, \quad (\text{B16})$$

$$\mathbf{C}(F_{\alpha\beta\gamma}|F_\alpha) = \mathbf{M}_{33} - \mathbf{M}_{13}^T 3\sigma_1^{-2} \mathbf{M}_{13}. \quad (\text{B17})$$

B3 Probability Function for Peaks

For the peaks, the original covariance matrix for the probability is represented in the 10 dimension vector $\mathbf{F}^{(10)}$. As presented by BBKS, we can see that the three degrees of freedom related to the directional dependence drop off from the parameter space for the homogeneous fields. After introduce the eigen coordinate, we can represent the peak number density in 7 dimension parameter space.

For convenience, we will introduce a new set of variables

$$\sigma_0 \nu = F, \quad (\text{B18})$$

$$\sigma_1 \nu_\alpha = F_\alpha, \quad (\text{B19})$$

$$\sigma_2 x = -\nabla^2 F = \lambda_1 + \lambda_2 + \lambda_3, \quad (\text{B20})$$

$$\sigma_2 y = \frac{(\lambda_1 - \lambda_3)}{2}, \quad (\text{B21})$$

$$\sigma_2 z = \frac{(\lambda_1 - 2\lambda_2 + \lambda_3)}{2}, \quad (\text{B22})$$

$$\begin{aligned}
dF_{\alpha\beta}^6 &= |(\lambda_1 - \lambda_2)(\lambda_2 - \lambda_3)(\lambda_1 - \lambda_3)| d\lambda_1 d\lambda_2 d\lambda_3 \\
&\quad \times d \text{vol}[SO(3)] \\
&= |2y(y^2 - z^2)| \frac{2}{3} \sigma_2^3 dx dy dz d \text{vol}[SO(3)], \quad (\text{B23})
\end{aligned}$$

where $d \text{vol}[SO(3)]$ is the volume element of the three-dimensional rotational group $SO(3)$. We had used the relations :

$$\lambda_1 = \frac{\sigma_2}{3}(x + 3y + z), \quad (\text{B24})$$

$$\lambda_2 = \frac{\sigma_2}{3}(x - 2z), \quad (\text{B25})$$

$$\lambda_3 = \frac{\sigma_2}{3}(x - 3y + z), \quad (\text{B26})$$

$$\prod_{i=1}^3 d\lambda_i = \frac{2}{3} \sigma_2^3 dx dy dz. \quad (\text{B27})$$

The probability function in these variables of $(F, F_\alpha, F_{\alpha\beta})$ is represented as that in the variables of (ν, η, x, y, z) with $\eta = (\nu_1, \nu_2, \nu_3)$.

$$P(F, F_\alpha, F_{\alpha\beta}) dF d^3 F_\alpha d^6 F_{\alpha\beta} =$$

$$\begin{aligned}
&P(\nu, \eta, x, y, z, \bar{\alpha}, \bar{\beta}, \bar{\gamma}) d\nu d^3 \eta \\
&\quad \times |2y(y^2 - z^2)| \frac{2}{3} \sigma_2^3 dx dy dz d \text{vol}[SO(3)], \quad (\text{B28})
\end{aligned}$$

where $\bar{\alpha}, \bar{\beta}, \bar{\gamma}$ are the Euler's angles. The directional dependence is not so important in the isotropic field. Then the mean of peak number density is enough to consider the statistics of the density field. The mean can be obtained by the angle independently integrations.

$$\begin{aligned}
&\int d \text{vol}[SO(3)] P(\nu, \eta, x, y, z, \bar{\alpha}, \bar{\beta}, \bar{\gamma}) \\
&= \frac{2\pi^2}{3!} P(\nu, \eta, x, y, z) \\
&= \frac{2\pi^2}{3!} P(x, y, z|\nu) P(\nu, \eta), \quad (\text{B29})
\end{aligned}$$

where we used $\int d \text{vol}[SO(3)] = 2\pi^2/3!$ with the degenerate of the triad orientation of the axis for the eigenvalues.

The determinant and the inverse of the conditional covariance matrix are given explicitly as

$$|\det \mathbf{C}(\nu_{\alpha\beta}|\nu)|^{1/2} = \frac{2}{5^{5/2} \cdot 3^3} (1 - \gamma^2)^{1/2}, \quad \gamma = \frac{\sigma_1^2}{\sigma_2 \sigma_0}, \quad (\text{B30})$$

where

$$\mathbf{C}(\nu_{\alpha\beta}|\nu)^{-1} = \begin{pmatrix} \frac{1}{1-\gamma^2} \mathbf{K}^{(3 \times 3)} + \mathbf{R} & \mathbf{0} \\ \mathbf{0} & -15\mathbf{I}^{(3 \times 3)} \end{pmatrix}, \quad (\text{B31})$$

$$\mathbf{R} = 5 \begin{pmatrix} 1 & -1/2 & -1/2 \\ -1/2 & 1 & -1/2 \\ -1/2 & -1/2 & 1 \end{pmatrix}. \quad (\text{B32})$$

The probability functions $P(x, y, z|\nu), P(\nu)$ are the same of that described by BBKS as

$$P(\nu, \eta) = \frac{3^{3/2}}{(2\pi)^2} \exp[-\frac{1}{2}(\nu^2 + 3\eta \cdot \eta)], \quad (\text{B33})$$

$$\begin{aligned}
P(x, y, z|\nu) &= \frac{3^3 \cdot 5^{5/2}}{(2\pi)^3 \cdot 2 \cdot (1 - \gamma^2)^{1/2}} \\
&\quad \times \exp[-\frac{1}{2}Q(x, y, z)], \quad (\text{B34})
\end{aligned}$$

$$Q(x, y, z) = \frac{(x - x_*)^2}{(1 - \gamma^2)} + 15y^2 + 5z^2, \quad x_* = \gamma\nu. \quad (\text{B35})$$

B4 Probability Function for Sloping Saddles

For the sloping saddles, in general, we should start from the original covariance matrix in the 20 dimension vector with 10 variables of the third derivatives of the field added to that for the peaks. After introduce the eigen coordinate, however, we need the third derivatives in only degenerate direction as the additional variables; $\nu_{3\alpha\alpha} = F_{3\alpha\alpha}/\sigma_3$. As similar as shown in the case of the peak, finally, the statistics of the sloping saddles of the homogeneous field can be determined in the parameter space $(\nu, \eta, x, y, z, \mathbf{w})$, where $\mathbf{w} = (w_1, w_2, w_3) = (\nu_{311}, \nu_{322}, \nu_{333})$. The conditional probability with the third derivatives of \mathbf{w} can be represented as

$$P(\mathbf{w}|\nu_3) = \frac{\exp[-\frac{1}{2}Q(\mathbf{w}|\nu_3)]}{(2\pi)^{3/2} |\det \mathbf{C}(\mathbf{w}|\nu_3)|^{1/2}}, \quad (\text{B36})$$

$$Q(\mathbf{w}|\nu_3) = \bar{\mathbf{w}}^T \mathbf{C}(\bar{\mathbf{w}}|\nu_3) \bar{\mathbf{w}}, \quad (\text{B37})$$

$$\bar{\mathbf{w}} = \mathbf{w} - \frac{-3}{5} \kappa \overline{\mathbf{M}}_{13} \nu_3, \quad (\text{B38})$$

$$\kappa = \frac{\sigma_2^2}{\sigma_3\sigma_1}. \quad (\text{B39})$$

The determinant and the inverse of the conditional covariance matrix for the variables $\bar{\nu}_{3\alpha\alpha}$ are represented as

$$|\det \mathbf{C}(\mathbf{w}|\nu_3)|^{1/2} = \frac{2}{5^{3/2} \cdot 3 \cdot 7} (1 - \kappa^2)^{1/2}, \quad (\text{B40})$$

$$\mathbf{C}(\mathbf{w}|\nu_3)^{-1} = \frac{1}{(1 - \kappa^2)} \begin{pmatrix} c_{11} & c_o & c_o \\ c_o & c_{22} & c_o \\ c_o & c_o & c_{33} \end{pmatrix}, \quad (\text{B41})$$

$$c_{11} = 10 - 7\kappa^2, \quad (\text{B42})$$

$$c_{22} = c_{33} = 45 - 42\kappa^2, \quad (\text{B43})$$

$$c_o = \frac{21\kappa^2 - 15}{2}. \quad (\text{B44})$$

With the condition of the first derivatives F_3 for the sloping saddles, we can represent the exponent part of the conditional probability:

$$Q(\mathbf{w}|\nu_3) = Q_1(w_1|w_2, w_3, \nu_3) + Q_2(w_2|w_3, \nu_3) + Q_3(w_3|\nu_3), \quad (\text{B45})$$

$$Q_1(w_1|w_2, w_3, \nu_3) = \frac{3(15 - 14\kappa^2)}{(1 - \kappa^2)} \times \left[\bar{w}_1 - \frac{(5 - 7\kappa^2)}{2(15 - 14\kappa^2)} \bar{w}_3 + \bar{w}_2 \right]^2, \quad (\text{B46})$$

$$Q_2(w_2|w_3, \nu_3) = \frac{3 \cdot 5 \cdot 7(25 - 21\kappa^2)}{2^2(15 - 14\kappa^2)} \times \left[\bar{w}_2 - \frac{(5 - 7\kappa^2)}{(25 - 21\kappa^2)} \bar{w}_3 \right]^2, \quad (\text{B47})$$

$$Q_3(w_3|\nu_3) = \frac{5^2 \cdot 7}{(25 - 21\kappa^2)} \bar{\nu}_{333}^2. \quad (\text{B48})$$

We will list up some integrations as

$$I_1 = \int_{-\infty}^{\infty} dw_1 \exp \left[-\frac{1}{2} Q_1(w_1|w_2, w_3, \nu_3) \right] = \frac{\sqrt{2\pi}(1 - \kappa^2)^{1/2}}{3^{1/2}(15 - 14\kappa^2)^{1/2}}, \quad (\text{B49})$$

$$I_2 = \int_{-\infty}^{\infty} dw_2 \exp \left[-\frac{1}{2} Q_2(w_2|w_3, \nu_3) \right] = \frac{2\sqrt{2\pi}(15 - 14\kappa^2)^{1/2}}{(3 \cdot 5 \cdot 7)^{1/2}(25 - 21\kappa^2)^{1/2}}, \quad (\text{B50})$$

$$I_{22} = \int_{-\infty}^{\infty} dw_2 w_2 \exp \left[-\frac{1}{2} Q_2(w_2|w_3, \nu_3) \right] = \int_{-\infty}^{\infty} dw_2 \frac{(5 - 7\kappa^2)}{(25 - 21\kappa^2)} \bar{w}_3 \exp \left[-\frac{1}{2} Q_2(w_2|w_3, \nu_3) \right] = \frac{(5 - 7\kappa^2)}{(25 - 21\kappa^2)} \bar{w}_3 I_2. \quad (\text{B51})$$

As shown in the definition of the sloping saddles, we are interested in mainly the probability for w_3 in the third derivative components. The conditional probability function of w_3 can be obtained from the integration with the other third derivative components w_1, w_2 as

$$P(w_3|\nu_3)dw_3 = \int_{-\infty}^{\infty} dw_1 \int_{-\infty}^{\infty} dw_2 P(\mathbf{w}|\nu_3) dw_3$$

$$= \frac{5^{3/2} \cdot 3 \cdot 7}{2(2\pi)^{3/2}(1 - \kappa^2)^{1/2}} \times I_1 \times I_2 \times \exp \left[-\frac{1}{2} \bar{Q}(w_3) \right] dw_3 = \frac{5 \cdot 7^{1/2}}{\sqrt{2\pi}(25 - 21\kappa^2)} \times \exp \left[-\frac{1}{2} \bar{Q}(w_3) \right] dw_3, \quad (\text{B52})$$

$$\bar{Q}(w_3) = \frac{5^2 \cdot 7}{(25 - 21\kappa^2)} (w_3 + \frac{3}{5}\kappa\nu_3)^2. \quad (\text{B53})$$

We can see the reasonable normalization in the integration of $P(w_3|\nu_3)$ with w_3 as

$$\int_{-\infty}^{\infty} dw_3 P(w_3|\nu_3) = 1. \quad (\text{B54})$$

For the convenience, we will represent the probability of w_3 with $\nu_3 = 0$;

$$P(w_3|\nu_3 = 0) = \frac{1}{\sqrt{2\pi}\sigma_w} \exp \left[-\frac{1}{2} \frac{w_3^2}{\sigma_w^2} \right], \quad (\text{B55})$$

$$\sigma_w^2 = \frac{(25 - 21\kappa^2)}{5^2 \cdot 7}. \quad (\text{B56})$$

We will calculate the integration required in the calculation of the instantaneous scale function of sloping saddles;

$$\int d^3 \mathbf{w} |w_3(w_1 + w_2 + w_3)| P(\mathbf{w}|\nu_3) = \langle w_3^2 \rangle_{ss} (1 + q_{ss}), \quad (\text{B57})$$

$$\langle w_3^2 \rangle_{ss} = \int_{-\infty}^{\infty} dw_3 (w_3)^2 P(w_3|\nu_3) = \frac{(25 - 21\kappa^2)}{5^2 \cdot 7}, \quad (\text{B58})$$

$$q_{ss} = \frac{(5 - 7\kappa^2)}{(25 - 21\kappa^2)}, \quad (\text{B59})$$

where we used

$$\int_{-\infty}^{\infty} dw_1 w_1 \int_{-\infty}^{\infty} dw_2 P(\mathbf{w}|\nu_3) dw_3 = \int_{-\infty}^{\infty} dw_2 w_2 \int_{-\infty}^{\infty} dw_1 P(\mathbf{w}|\nu_3) dw_3 = q_{ss} \bar{w}_3 P(w_3|\nu_3) dw_3. \quad (\text{B60})$$

APPENDIX C: CALCULATIONS OF SCALE FUNCTIONS

C1 Ensemble Averaged Density of Peaks

The constraint of the peaks can be rewritten to

$$C(\mathbf{F}^{(10)}|\text{peaks}) = |\lambda_1 \lambda_2 \lambda_3| \prod_{\alpha=1}^3 \delta(F_\alpha) \Theta(\lambda_3) = \frac{(x - 2z)[(x + z)^2 - y^2]}{3^3} \left(\frac{\sigma_2}{\sigma_1}\right)^3 \times \prod_{\alpha=1}^3 \delta(\nu_\alpha) \Theta(x - 2z). \quad (\text{C1})$$

With the constraint, in order to derive the ensemble-averaged number density of peaks, we will start from its probability weighted number density:

$$\begin{aligned} n_{pk}(\nu, x, y, z; R) d\nu dx dy dz \\ = 6 \cdot P(\nu, \eta = \mathbf{0}, x, y, z) C(\mathbf{F}^{(10)} | \text{peaks}) d\nu dx dy dz \\ = \frac{5^{5/2} 3^{1/2}}{(2\pi)^3} \left(\frac{\sigma_2}{\sigma_1}\right)^3 \frac{\exp[-\frac{1}{2}\nu^2] \exp[-\frac{1}{2}Q(x, y, z)]}{\sqrt{1-\gamma^2}} \\ \times \psi_{pk}(x, y, z) \phi_{pk}(x, y, z) d\nu dx dy dz, \quad (C2) \end{aligned}$$

$$\begin{aligned} \psi_{pk}(x, y, z) &= \frac{3^3}{2} \sigma_2^{-6} \lambda_1 \lambda_2 \lambda_3 (\lambda_1 - \lambda_2) (\lambda_2 - \lambda_3) (\lambda_1 - \lambda_3) \\ &= (x - 2z)[(x + z)^2 - (3y)^2] y (y^2 - z^2) \quad (C3) \end{aligned}$$

$$\phi_{pk}(x, y, z) = \begin{cases} 1 & \text{if } \frac{x}{4} \geq y \geq 0 \text{ and} \\ & -y \geq z \geq y \\ 1 & \text{if } \frac{x}{2} \geq y \geq \frac{x}{4} \text{ and} \\ & 3y - x \geq z \geq y \\ 0 & \text{otherwise} \end{cases},$$

where $\phi(x, y, z)$ is the condition of $\lambda_i > 0$ and we had multiplied the probability expression by 6 to account for the ordering of the eigenvalues of λ_i .

After the integration over y, z , the ensemble-averaged density of the peaks is given as

$$\begin{aligned} \langle n_{pk}(\nu, x; R) \rangle d\nu dx &= \frac{\exp[-\frac{1}{2}\nu^2]}{(2\pi)^2 R_*^3} d\nu \\ &\times f_{pk}(x) \frac{\exp[-(x-x_*)^2/2(1-\gamma^2)]}{\sqrt{2\pi(1-\gamma^2)}} dx, \quad (C4) \end{aligned}$$

where $R_* = \sqrt{3} \frac{\sigma_1}{\sigma_2}$ and

$$\begin{aligned} f_{pk}(x) &= \frac{3^2 5^{5/2}}{\sqrt{2\pi}} \left[\int_0^{x/4} dy e^{-15y^2/2} \int_{-y}^y \psi_{pk}(x, y, z) dz e^{-5z^2/2} \right. \\ &+ \left. \int_{x/4}^{x/2} dy e^{-15y^2/2} \int_{3y-x}^y \psi_{pk}(x, y, z) dz e^{-5z^2/2} \right], \\ &= \frac{(x^3 - 3x)}{2} \{ \text{Erf}[(5/2)^{1/2} x] + \text{Erf}[(5/2)^{1/2} \frac{x}{2}] \} \\ &+ \left(\frac{2}{5\pi}\right)^{1/2} \left[\left(\frac{31x^2}{4} + \frac{8}{5}\right) e^{-5x^2/8} \right. \\ &\left. + \left(\frac{x^2}{2} - \frac{8}{5}\right) e^{-5x^2/2} \right]. \quad (C5) \end{aligned}$$

The density of the peaks of ν at the scale R can be represented as

$$\langle n_{pk}(\nu; R) \rangle d\nu = \frac{\exp(-\frac{1}{2}\nu^2)}{(2\pi)^2 R_*^3} G_{pk}(\gamma, x_*) d\nu, \quad (C6)$$

where

$$G_{pk}(\gamma, x_*) = \int_0^\infty dx f_{pk}(x) \frac{\exp[-(x-x_*)^2/2(1-\gamma^2)]}{\sqrt{2\pi(1-\gamma^2)}} d\nu. \quad (C7)$$

The function $G_{pk}(\gamma, x_*)$ have a following fitting formula obtained by BBKS,

$$G_{pk}(\gamma, x_*) \simeq \frac{w^3 - 3\gamma^2 w + [Bw^2 + C_1] \exp[-Aw^2]}{1 + C_2 \exp[-C_3 w]}, \quad (C8)$$

$$A = \frac{5/2}{(9 - 5\gamma^2)}, \quad (C9)$$

$$B = \frac{432}{(10\pi)^{1/2} (9 - 5\gamma^2)^{5/2}}, \quad (C10)$$

$$C_1 = 1.84 + 1.13(1 - \gamma^2)^{5.72}, \quad (C11)$$

$$C_2 = 8.91 + 1.27 \exp(6.51\gamma^2), \quad (C12)$$

$$C_3 = 2.58 \exp(1.05\gamma^2). \quad (C13)$$

We also have the averaged x ;

$$\begin{aligned} H_{pk}(\gamma, x_*) &= \int_0^\infty x dx f_{pk}(x) \\ &\times \left\{ \frac{\exp[-(x-x_*)^2/2(1-\gamma^2)]}{\sqrt{2\pi(1-\gamma^2)}} \right\} \\ &= \langle x \rangle_{pk} G_{pk}(\gamma, x_*). \quad (C14) \end{aligned}$$

We can easily see that the mean value $\langle x \rangle_{pk}$ is $H_{pk}(\gamma, x_*)/G_{pk}(\gamma, x_*)$, which can be also represented as a approximated form as derived by BBKS :

$$\langle x \rangle_{pk} = \gamma\nu + \theta(\gamma, \gamma\nu), \quad (C15)$$

$$\theta(\gamma, \gamma\nu) = \frac{\theta_1 + \theta_2 \exp[-\gamma/2(\gamma\nu/2)^2]}{[\theta_1 + 0.45 + (\gamma\nu/2)^2]^{1/2} + \gamma\nu/2}, \quad (C16)$$

$$\theta_1 = 3(1 - \gamma^2), \theta_2 = (1.216 - 0.9\gamma^4). \quad (C17)$$

C2 Scale Functions of Peaks

The calculated ensemble-averaged densities is equal to them of BBKS as

$$\langle n_{pk}(\nu, x; R) \rangle dx d\nu = \mathcal{N}_{pk}(\nu, x; R) dx d\nu. \quad (C18)$$

With transformation of the density contrast ν to the resolution scale R , we can obtain the scale function of peaks:

$$\begin{aligned} N_{pk}(R, x, \delta_c) dR dx &= \mathcal{N}_{pk}(\nu, x; R) x \left(\frac{\sigma_2}{\sigma_0}\right) R dR dx \\ &= \frac{\exp[-\frac{1}{2}\nu^2]}{(2\pi)^2 R_*^3} x \frac{\sigma_2(R)}{\sigma_0(R)} R dR \\ &\times f_{pk}(x) \frac{\exp[-(x-x_*)^2/2(1-\gamma^2)]}{\sqrt{2\pi(1-\gamma^2)}} dx. \quad (C19) \end{aligned}$$

This is the scale function of the peaks with the parameter of x . With the integration of x , the density function of peaks satisfying the condition of collapse threshold δ_c is given as

$$\begin{aligned} N_{pk}(R, \delta_c) dR &= \int_0^\infty x dx \mathcal{N}_{pk}(\nu_c, x, R) \frac{\sigma_2(R)}{\sigma_0(R)} R dR \\ &= \frac{H_{pk}(\gamma, x_*)}{(2\pi)^2 R_*^3} \exp[-\frac{1}{2}\nu_c^2] \frac{\sigma_2(R)}{\sigma_0(R)} R dR \\ &= \mathcal{N}_{pk}(\nu_c, R) \langle x \rangle_{pk} \frac{\sigma_2(R)}{\sigma_0(R)} R dR. \quad (C20) \end{aligned}$$

C3 Scale Functions of The Nesting and Non-Nesting Peaks

The above peak counting does not distinct nesting peaks and non-nesting peaks. In order to count the nesting peaks, we will introduce the joint scale function of the nesting peaks :

$$\begin{aligned} N_{pk}^{nest}(R_b, R_s; \delta_c) dR_b dR_s &= N_{pk}^{nest}(R_s, |R_b; \delta_c) dR_s \\ &\times f(R_b, \delta_c) dR_b \quad (C21) \end{aligned}$$

where the fraction of the volume occupation with the objects related to the filtering scale R_l is given as

$$f(R, \delta) dR = \text{Vol}(R) N(R, \delta) dR, \quad (C22)$$

$$\text{Vol}(R) = \frac{M(R)}{\rho}, \quad (\text{C23})$$

where $N(R, \delta)dR$ is the scale function of non-nesting peaks.

In general, the conditional density of the peaks at δ_s within the background at δ_b on the larger scale R_b can be expressed as

$$\begin{aligned} N_{pk}^{nest}(R_s, \delta_s | R_b, \delta_b) dR_s = \\ N_{pk}(R_s, \delta_s | R_b, \delta_b) \frac{\sigma_2(R_s)}{\sigma_0(R_s)} \langle \tilde{x} \rangle_{R_s} dR_s, \end{aligned} \quad (\text{C24})$$

in terms of the conditional density $N_{pk}(R_s, \delta_s | R_b, \delta_b)$ obtained by BBKS. Here, the function $\langle \tilde{x} \rangle = \langle x \rangle_{pk}(\tilde{\gamma}, \tilde{x}_*)$, where

$$\tilde{x}_* = \tilde{\gamma} \tilde{\nu}, \quad \tilde{\gamma} = \gamma \sqrt{1 + \epsilon^2 \frac{(1-r_1)^2}{1-\epsilon^2}}, \quad (\text{C25})$$

$$\tilde{\nu} = \frac{\gamma}{\tilde{\gamma}} \left(\frac{1-r_1}{1-\epsilon^2} \right) \left[\nu_s \left(\frac{1-\epsilon^2 r_1}{1-r_1} \right) - \epsilon \nu_b \right]. \quad (\text{C26})$$

The subscripts b , s and h mean the values of the scales R_b , R_s , and R_h ($R_b > R_h > R_s$). According to BBKS, we introduced the following notations;

$$\epsilon = \frac{\sigma_{0h}^2}{\sigma_{0b}\sigma_{0s}}, \quad (\text{C27})$$

$$r_1 = \frac{\langle k^2 \rangle_h}{\langle k^2 \rangle_s} = \frac{\sigma_{1h}^2 \sigma_{0s}^2}{\sigma_{0h}^2 \sigma_{1s}^2} = \frac{\sigma_{2h} \sigma_{0s}}{\sigma_{0h} \sigma_{2s}}, \quad (\text{C28})$$

$$r_2 = \frac{\langle k^3 \rangle_h}{\langle k^3 \rangle_s} = \frac{\sigma_{1h}^3 \sigma_{0s}^3}{\sigma_{0h}^3 \sigma_{1s}^3} = \frac{\sigma_{3h} \sigma_{0s}}{\sigma_{0h} \sigma_{3s}}, \quad (\text{C29})$$

$$\sigma_{jh} = 4\pi \int dk k^{2j+2} |\delta_k|^2 W(k; R_b) W(k; R_s). \quad (\text{C30})$$

Since we use the Gaussian filter, we can rewrite as $\sigma_{jh} = \sigma_j(R_h)$ with the rms average $R_h = [(R_b^2 + R_s^2)/2]^{1/2}$.

This conditional density of peaks gives a form for $N_{pk}^{nest}(R_s, |R_b; \delta_c) dR_s$ at the the limit of $\delta_b \rightarrow \delta_s = \delta_s$. In this paper, we use this simple form for the conditional density as

$$\begin{aligned} N_{pk}^{nest}(R_s, |R_b; \delta_c) dR_s = \\ N_{pk}(R_s, \delta_c | R_b, \delta_c) \frac{\sigma_2(R_s)}{\sigma_0(R_s)} \langle \tilde{x} \rangle_{R_s} dR_s. \end{aligned} \quad (\text{C31})$$

The number density of the non-nesting peaks $N(R, \delta_c)$ can be obtained by subtracting the density of the pairs of nesting peaks $N^{nest}(R, \delta_c)$ from that of all peaks $N_{pk}(R, \delta_c)$, which includes the nesting peaks $N^{nest}(R, \delta_c)$ at δ_c on the scale R . Then, the notations to the corrected scale function is

$$N(R, \delta_c) dR = N_{pk}(R, \delta_c) dR - N^{nest}(R, \delta_c) dR. \quad (\text{C32})$$

The scale function of the nesting peaks can be calculated from the integration of the joint scale function of the nesting peaks $N^{nest}(R, R'; \delta_c) dR_c d\delta_c$,

$$\begin{aligned} N^{nest}(R, \delta_c) dR &= \int_R^\infty dR' N^{nest}(R', R; \delta_c) dR_c \\ &= \int_R^\infty dR' f(R', \delta_c) \\ &\quad \times N_{pk}^{nest}(R | R'; \delta_c) dR. \end{aligned} \quad (\text{C33})$$

This is a Volterra type integral equation, which can be solved

with the iteration process in exact mean as shown in Manrique & Salvador-Sole (1995). The number density of the non-nesting peaks $N(R, \delta_c)$ can be also obtained with the same iteration process. The number density of the nesting peaks can be negligible to that of all peaks, as shown in Fig. 2.

C4 Ensemble Averaged Density of Sloping Saddles

The constraint of the sloping saddles are rewritten to

$$\begin{aligned} C(\mathbf{F}^{(20)} | \text{s. saddles}) dR = \\ \frac{1}{3} \frac{\sigma_2 \sigma_3}{\sigma_1^2} |(x+3y+z)(x-2z)w_3(w_1+w_2+w_3)| \\ \times \delta(z-3y+x) \delta^{(3)}(\eta) \left(\frac{\sigma_3}{\sigma_1} \right) R dR. \end{aligned} \quad (\text{C34})$$

With the constraint, the probability weighted number density of the sloping saddles is represented as

$$\begin{aligned} \mathbf{n}_{ss}(\nu, x, y, z, \mathbf{w}; R) d\nu dx dy dz d^3 \mathbf{w} dR \\ = 6 \cdot P(\mathbf{w} | \nu_3 = 0) d^3 \mathbf{w} P(x, y, z | \nu) dx dy dz P(\nu, \eta = 0) d\nu \\ \times C(\mathbf{F}^{(20)} | \text{s. saddles}) dR \\ = \frac{3^{5/2} \cdot 5^{5/2}}{(2\pi)^3} \left(\frac{\sigma_2 \sigma_3}{\sigma_1^2} \right) R \psi_{ss}(x, y, z) \phi_{ss}(x, y, z) \\ \times \frac{\exp[-\frac{1}{2}\nu^2] \exp[-\frac{1}{2}Q(x, y, z)]}{\sqrt{1-\gamma^2}} d\nu dx dy dz \\ \times |w_3(w_1+w_2+w_3)| P(\mathbf{w} | \nu_3 = 0) d^3 \mathbf{w} \\ \times \left(\frac{\sigma_3}{\sigma_1} \right) R dR, \end{aligned} \quad (\text{C35})$$

$$\begin{aligned} \psi_{ss}(x, y, z) &= y(y^2 - z^2)(x + 3y + z) \\ &\quad \times (x - 2z) \delta(z - 3y + x), \end{aligned} \quad (\text{C36})$$

$$\phi_{ss}(x, y, z) = \phi_{pk}(x, y, z), \quad (\text{C37})$$

where the factor 6 is needed to account for the ordering of λ_i the same as that of the peaks. With the integration over y, z , we can obtain the density of the sloping saddles similar to that of the peaks;

$$\begin{aligned} \langle \mathbf{n}_{ss}(\nu, x, \mathbf{w}; R) \rangle d\nu dx d^3 \mathbf{w} dR \\ = \frac{\exp[-\frac{1}{2}\nu^2] d\nu}{(2\pi)^2 R_*^3} \\ \times f_{ss}(\kappa, x) \frac{\exp[-(x-x_*)^2/2(1-\gamma^2)]}{\sqrt{2\pi(1-\gamma^2)}} dx \\ \times |w_3(w_1+w_2+w_3)| P(\mathbf{w} | \nu_3 = 0) d^3 \mathbf{w} \\ \times \left(\frac{\sigma_3}{\sigma_1} \right) R dR, \end{aligned} \quad (\text{C38})$$

where we used the relation $(\sigma_2 \sigma_3 / \sigma_1^2)^{1/3} = \sqrt{3} / \kappa^{1/3} / R_*$, and

$$\begin{aligned} f_{ss}(\kappa, x) &= A_{ss}(\kappa) \int_{x/4}^{x/2} dy \mathcal{Y}(y; x) \\ &= A_{ss}(\kappa) e^{-5x^2/8} \left[\frac{4}{5^3 \cdot 3} (1 - e^{-15x^2/8}) \right. \\ &\quad \left. + \frac{1}{5} x^2 \left(\frac{3x^2}{2^5} - \frac{1}{10} \right) \right], \end{aligned} \quad (\text{C39})$$

$$A_{ss}(\kappa) = \frac{3^4 \cdot 5^{5/2}}{\sqrt{2\pi\kappa}}, \quad (\text{C40})$$

$$\begin{aligned} \mathcal{Y}(y; x) &= e^{-15y^2/2} \int_{3y-x}^y \psi_{ss}(x, y, z) e^{-5z^2/2} dz \\ &= 18y^2(x-2y)^2(4y-x) \\ &\quad \times \exp\left[-\frac{15y^2}{2} - \frac{5(3y-x)^2}{2}\right]. \end{aligned} \quad (\text{C41})$$

The density averaged with \mathbf{w} is given

$$\begin{aligned} \langle \mathbf{n}_{ss}(\nu, x; R) \rangle dR dx d\nu &= \frac{\exp[-\frac{1}{2}(\nu^2)] d\nu}{(2\pi)^2 R_*^3} \\ &\times f_{ss}(x) \frac{\exp[-\frac{(x-x_*)^2}{2(1-\gamma^2)}]}{\sqrt{2\pi(1-\gamma^2)}} dx \\ &\times \langle w^2 \rangle_{ss} (1+q_{ss}) \frac{\sigma_3(R)}{\sigma_1(R)} R dR. \end{aligned} \quad (\text{C42})$$

With the integration over x , the averaged density is

$$\begin{aligned} \langle \mathbf{n}_{ss}(\nu; R) \rangle dR d\nu &= \frac{G_{ss}(\gamma, x_*) e^{-\frac{1}{2}\nu^2}}{(2\pi)^2 R_*^3} d\nu \\ &\times \langle w^2 \rangle_{ss} (1+q_{ss}) \frac{\sigma_3(R)}{\sigma_1(R)} R dR, \end{aligned} \quad (\text{C43})$$

where

$$G_{ss}(\gamma, \kappa, x_*) = \int_0^\infty f_{ss}(x) \frac{\exp[-\frac{(x-x_*)^2}{2(1-\gamma^2)}]}{\sqrt{2\pi(1-\gamma^2)}} dx. \quad (\text{C44})$$

The exact result of the integration is obtained as an analytical form

$$\begin{aligned} G_{ss}(\gamma, \kappa, x_*) &= \frac{A_{ss}(\kappa)}{\sqrt{2\pi(1-\gamma^2)}} \left[\frac{2(1-\gamma^2)x_*}{5(9-5\gamma^2)^3} \left\{ \frac{12x_*^2}{(9-5\gamma^2)} + \frac{(39-55\gamma^2)}{5} \right\} e^{-\frac{x_*^2}{2(1-\gamma^2)}} \right. \\ &+ \sqrt{\frac{2\pi(1-\gamma^2)}{(9-5\gamma^2)^9}} \left\{ \frac{24x_*^4}{5} + \frac{4(27-35\gamma^2)(9-5\gamma^2)x_*^2}{25} \right. \\ &\quad \left. \left. + \frac{(783-1230\gamma^2+575\gamma^4)(9-5\gamma^2)^2}{750} \right\} \right. \\ &\quad \times \left\{ 1 + \text{Erf} \left[x_* \sqrt{\frac{2}{(9-5\gamma^2)(1-\gamma^2)}} \right] \right\} e^{-\frac{5x_*^2}{2(9-5\gamma^2)}} \\ &- \frac{2}{375} \sqrt{\frac{2\pi(1-\gamma^2)}{(6-5\gamma^2)}} \left\{ 1 + \text{Erf} \left[\frac{x_*}{\sqrt{2(6-5\gamma^2)(1-\gamma^2)}} \right] \right\} \\ &\quad \left. \times e^{-\frac{5x_*^2}{2(6-5\gamma^2)}} \right]. \end{aligned} \quad (\text{C45})$$

The mean value of x at the sloping saddles is

$$\langle x \rangle_{ss} = \frac{H_{ss}(\gamma, \kappa, x_*)}{G_{ss}(\gamma, \kappa, x_*)}, \quad (\text{C46})$$

$$H_{ss}(\gamma, \kappa, x_*) = \int_0^\infty x f_{ss}(x) \frac{\exp[-\frac{(x-x_*)^2}{2(1-\gamma^2)}]}{\sqrt{2\pi(1-\gamma^2)}} dx, \quad (\text{C47})$$

where we can also obtain the analytical result of the integration :

$$H_{ss}(\gamma, \kappa, x_*) = \frac{A_{ss}(\kappa)}{\sqrt{2\pi(1-\gamma^2)}} \left[\right.$$

$$\begin{aligned} &\frac{4(1-\gamma^2)}{(9-5\gamma^2)^3} \left\{ \frac{24x_*^4}{5(9-5\gamma^2)^2} + \frac{2(99-115\gamma^2)x_*^2}{25(9-5\gamma^2)} \right. \\ &\quad \left. + \frac{9(1-\gamma^2)^3}{6-5\gamma^2} \right\} e^{-\frac{x_*^2}{2(1-\gamma^2)}} \\ &+ \frac{2}{5} \sqrt{\frac{2\pi(1-\gamma^2)}{(9-5\gamma^2)^7}} \left\{ \frac{48x_*^5}{(9-5\gamma^2)^2} + \frac{8(57-65\gamma^2)x_*^3}{5(9-5\gamma^2)} \right. \\ &\quad \left. + \frac{(2403-4950\gamma^2+2675\gamma^4)x_*}{75} \right\} \\ &\quad \times \left\{ 1 + \text{Erf} \left[x_* \sqrt{\frac{2}{(9-5\gamma^2)(1-\gamma^2)}} \right] \right\} x_* e^{-\frac{5x_*^2}{2(9-5\gamma^2)}} \\ &- \frac{2}{375} \sqrt{\frac{2\pi(1-\gamma^2)}{(6-5\gamma^2)^3}} \left\{ 1 + \text{Erf} \left[x_* \frac{1}{\sqrt{2(6-5\gamma^2)(1-\gamma^2)}} \right] \right\} \\ &\quad \times x_* e^{-\frac{5x_*^2}{2(6-5\gamma^2)}} \left. \right] \end{aligned} \quad (\text{C48})$$

APPENDIX D: SOME FORMULA IN THE CASES FOR POWER LAW SPECTRUM

When the power spectrum can be represented as a simple power law as

$$|\delta_k|^2 = Ak^n, \quad (\text{D1})$$

we can obtain the useful relations for the calculations as

$$\sigma_j(R) = A^{1/2} \sqrt{2\pi} R^{-(\frac{n+3}{2}+j)} \Gamma\left(\frac{n+3}{2}+j\right)^{1/2}, \quad (\text{D2})$$

$$\frac{\sigma_i(R)^2}{\sigma_j(R)^2} = \frac{(2i+n+1)!!}{2^{i-j}(2j+n+1)!!} R^{-2(i-j)}, \quad (\text{D3})$$

$$R_* = \left(\frac{6}{n+5}\right)^{1/2} R, \quad (\text{D4})$$

$$\gamma^2 = \left(\frac{\sigma_1^2}{\sigma_0\sigma_2}\right)^2 = \left(\frac{n+3}{n+5}\right), \quad (\text{D5})$$

$$\kappa^2 = \left(\frac{\sigma_2^2}{\sigma_1\sigma_3}\right)^2 = \left(\frac{n+5}{n+7}\right), \quad (\text{D6})$$

$$\epsilon = \left(\frac{R_s R_b}{R_h^2}\right)^{(n+3)/2}, \quad (\text{D7})$$

$$r_1 = \left(\frac{R_s}{R_h}\right)^2, \quad (\text{D8})$$

$$r_2 = \left(\frac{R_s}{R_h}\right)^3. \quad (\text{D9})$$